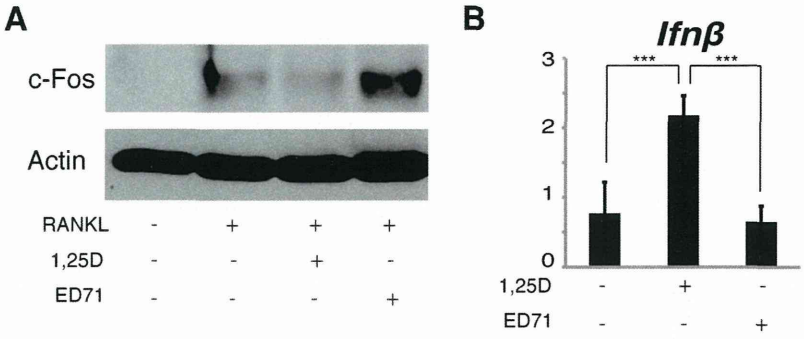

Figure 2. 1,25(OH)$_2$D$_3$ is more active in promoting c-Fos protein inhibition and *Ifnβ*-induction in osteoclasts compared with ED71. (A and B) M-CSF-dependent osteoclast progenitor cells were isolated from wild-type mice and cultured in the presence of M-CSF alone (50 ng/ml) or M-CSF + RANKL (25 ng/ml) with or without 10^{-7} M ED71 or 1,25(OH)$_2$D$_3$ (1,25D) for 5 days. c-Fos protein was then assessed by western blot (A). *Ifnβ* expression was analyzed by realtime PCR (B). Data represent mean *Ifnβ* expression relative to that of *Actb* ± SD ($n = 5$). ***$P<0.001$.
doi:10.1371/journal.pone.0111845.g002

Corp.). For chemical treatment, cells were cultured in phenol red-free media containing 10% charcoal-stripped FBS (Thermo Fisher Scientific K.K., Yokohama, Japan), and treated with 1,25(OH)$_2$D$_3$ (Wako Pure Chemicals Industries, Osaka, Japan, 10^{-7} M) or ED71 (provided by Chugai Pharmaceutical Co., Ltd, Tokyo, Japan, 10^{-7} M). Hypoxic cultures was performed at 5% O_2/5% CO_2 using an INVIVO2 hypoxia workstation (Ruskin Technology Ltd., Bridgend, UK) according to manufacturer's instruction.

Quantitative PCR analysis

Total RNA was isolated from bone marrow cultures using an RNeasy mini kit (Qiagen), and cDNA synthesis was done by using oligo (dT) primers and reverse transcriptase (Wako Pure Chemicals Industries). Quantitative PCR was performed using SYBR Premix ExTaq II reagent and a DICE Thermal cycler (Takara Bio Inc., Shiga, Japan), according to the manufacturer's instructions. *β-actin* (*Actb*) expression served as an internal control. Primers for *Nfatc1*, *Ctsk*, *DC-STAMP*, *Ifnβ* and *Actb* were as follows.

Ctsk-forward: 5′-ACGGAGGCATTGACTCTGAAGATG-3′

Ctsk-reverse: 5′-GGAAGCACCAACGAGAGGAGAAAT-3′

NFATc1-forward: 5′-CAAGTCTCACCACAGGGCTCACT-A-3′

NFATc1-reverse: 5′-GCGTGAGAGGTTCATTCTCCAAG-T-3′

DC-STAMP-forward: 5′-TCCTCCATGAACAAACAGTTC-CAA-3′

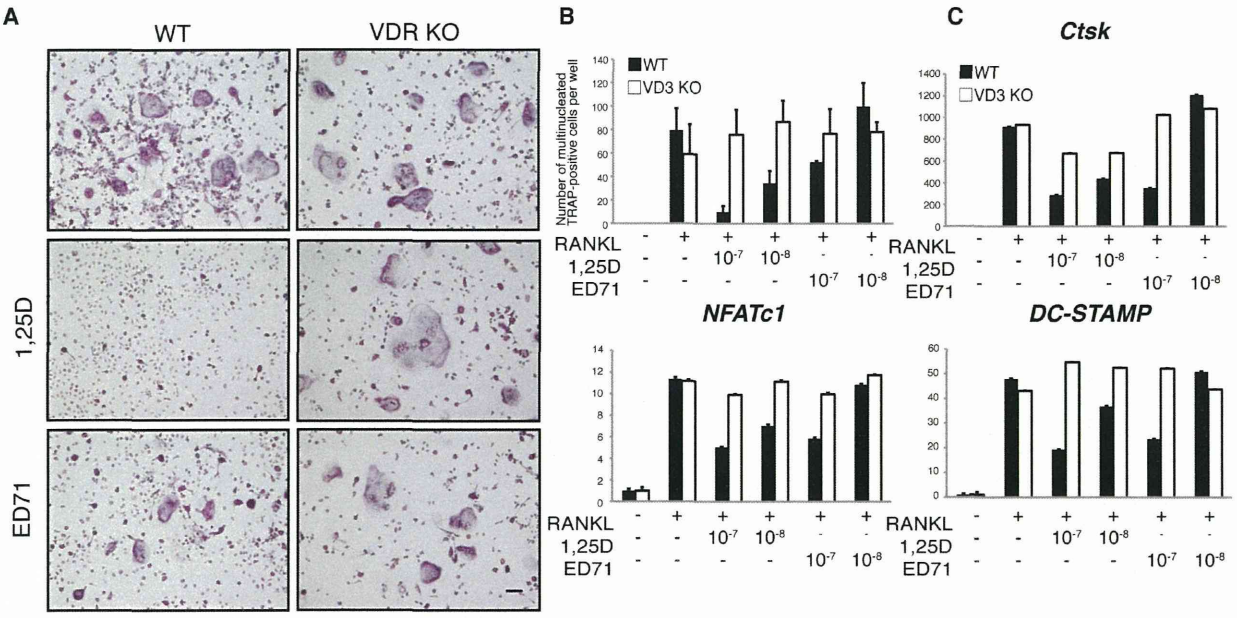

Figure 3. ED71 or 1,25(OH)$_2$D$_3$ activity requires the VDR. (**A, B** and **C**) M-CSF-dependent osteoclast progenitor cells were isolated from wild-type (WT) or VDR-deficient (VDR KO) mice and cultured in the presence of M-CSF alone (50 ng/ml) or M-CSF + RANKL (25 ng/ml) with or without indicated concentrations of ED71 or 1,25(OH)$_2$D$_3$ for 5 days. Cells were then stained with TRAP (**A**), and multi-nuclear TRAP-positive cells were counted (**B**). Expression of *Ctsk*, *NFATc1* and *DC-STAMP* was assessed by realtime PCR (**C**). Data represent mean *Ctsk*, *NFATc1* or *DC-STAMP* expression relative to that of *Actb* ± SD ($n = 5$).
doi:10.1371/journal.pone.0111845.g003

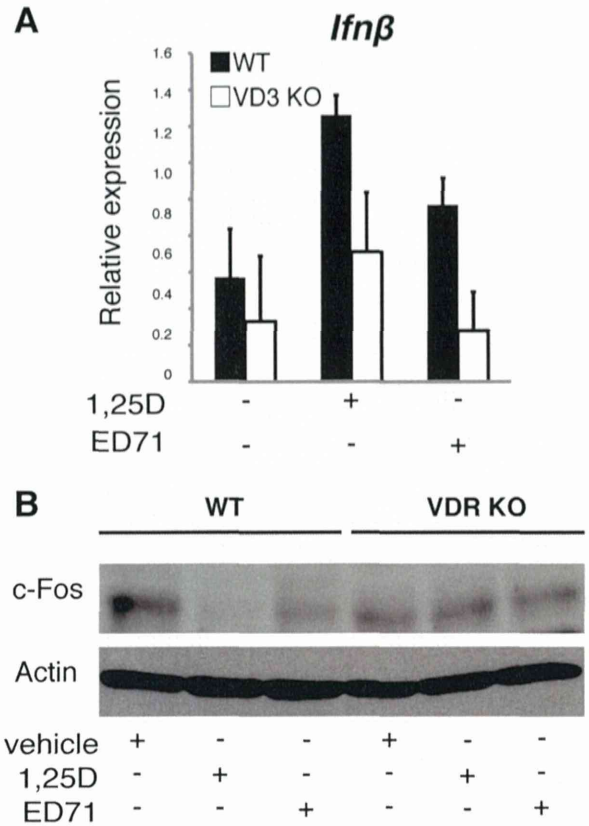

Figure 4. ED71 or $1,25(OH)_2D_3$ induce *Ifnβ* and suppress c-Fos protein through the VDR. (**A** and **B**) M-CSF-dependent osteoclast progenitor cells were isolated from wild-type or VDR-deficient mice and cultured in the presence of M-CSF alone (50 ng/ml) or M−CSF + RANKL (25 ng/ml) with or without 10^{-7} M of ED71 or $1,25(OH)_2D_3$ (1,25D) for 5 days. *Ifnβ* expression was then analyzed by realtime PCR (**A**). Data represent mean *Ifnβ* expression relative to that of *Actb* ± SD ($n = 5$). c-Fos protein was analyzed by western blot (**B**).
doi:10.1371/journal.pone.0111845.g004

DC-STAMP-reverse: 5′-AGACGTGGTTTAGGAATGCAG-CTC-3′
Ifnβ-forward: 5′– AAAGCAAGAGGAAAGATTGACGTG -3′
Ifnβ-reverse: 5′– ATCCAGGCGTAGCTGTTGTACTTC -3′
Blimp1-forward: 5′-TTCTTGTGTGGTATTGTCGGGAC-TT-3′
Blimp1-reverse: 5′-TTGGGGACACTCTTTGGGTAGAGT-T-3′
Irf8-forward: 5′-CAGGATTACAATCAGGAGGTGGA-3′
Irf8-reverse: 5′-TCAAAATCTGGGCTCTTGTTCAG-3′
β-actin-forward: 5′-TGAGAGGGAAATCGTGCGTGAC-3′
β-actin-reverse: 5′-AAGAAGGAAGGCTGGAAAAGAG-3′

Immunoblotting

Whole cell lysates were prepared using RIPA buffer (1% Triton X-100, 1% sodium deoxycholate, 0.1% SDS, 150 mM NaCl, 5 mM EDTA, 1 mM dithiothreitol, 10 mM Tris-HCl, pH 7.5) supplemented with a protease inhibitor cocktail (Sigma-Aldrich Co.) and MG-132 (EMD Millipore Corporation). The insoluble fraction was removed by centrifugation followed. Equivalent amounts of protein were separated by SDS-PAGE and transferred to a PVDF membrane (EMD Millipore Corporation). Proteins were detected using the following antibodies: anti-Fos (Santa Cruz Biotechnology, Santa Cruz, CA, USA), anti-HIF1α (Novus Biologicals, Littleton, CO, USA), anti-Actin(Sigma-Aldrich Co.), and anti-Vinculin (Sigma-Aldrich Co.) as previously described [14].

VDR knockdown

Raw264.7 cells transduced with MISSION shRNA lentiviruses targeting the VDR or with lentiviruses harboring non-target control constructs (Sigma-Aldrich Co.) were generated according to the manufacturer's instructions.

Statistical analyses

Statistical analyses were performed using an unpaired two-tailed Student's *t*-test (*$P<0.05$; **$P<0.01$; ***$P<0.005$; NS, not significant, throughout the paper). All data are expressed as the mean ± SD.

Results

$1,25(OH)_2D_3$ inhibits osteoclastogenesis more potently than does ED71 *in vitro*

Since treatment with ED71, a vitamin D3 analogue, inhibits osteoclast activity and increases bone mineral density more effectively than does the pro-$1,25(OH)_2D_3$ agent, alfacalcidol [12], we asked whether ED71 inhibited osteoclastogenesis more effectively than $1,25(OH)_2D_3$ (1,25D) *in vitro* (Fig. 1). To do so, we isolated osteoclast progenitor cells from wild-type mice and cultured them in the presence of M-CSF and RANKL with or without ED71 or $1,25(OH)_2D_3$. We then evaluated osteoclastogenesis by counting multi-nuclear TRAP-positive osteoclasts and examining expression of osteoclastic genes (Fig. 1A-D). Indeed ED71 significantly inhibited osteoclast differentiation based on both TRAP and gene expression analysis, while $1,25(OH)_2D_3$ was more effective in inhibiting osteoclastogenesis than was ED71 *in vitro* (Fig. 1A and B). Expression of osteoclast differentiation markers such as *Cathepsin K* (*Ctsk*), *nuclear factor of activated T cells 1* (*NFATc1*) and *dendritic cell specific transmembrane protein* (*DC-STAMP*) was more significantly inhibited by $1,25(OH)_2D_3$ than by ED71 treatment (Fig. 1C). Induction of B lymphocyte-induced maturation protein 1 (Blimp1) followed by suppression of B cell lymphoma 6 and interferon regulatory factor 8 (Irf8) is reportedly required for osteoclastogenesis [14,17,18]. We found that treatment of osteoclast progenitors with $1,25(OH)_2D_3$ elicited more robust inhibition of *Blimp1* and activation of *Bcl6* and *Irf8* than did treatment with ED71 (Fig. 1D), suggesting that $1,25(OH)_2D_3$ is more potent in inhibiting osteoclastogenesis induced by M-CSF and RANKL than ED71.

$1,25(OH)_2D_3$ reportedly inhibits osteoclast differentiation induced by M-CSF and RANKL by inhibiting c-Fos protein expression *in vitro* [10]. We found that, by western blot, c-Fos protein was induced by RANKL, and ED71 did not suppress c-Fos protein in osteoclasts as effectively as did $1,25(OH)_2D_3$ (Fig. 2A). Although $1,25(OH)_2D_3$ reportedly inhibits osteoclastogenesis induced by M-CSF and RANKL via *Ifnβ* induction *in vitro* [11], we found that, unlike $1,25(OH)_2D_3$, ED71 did not induce *Ifnβ* expression in osteoclasts (Fig. 2B).

The VDR is required for both $1,25(OH)_2D_3$ and ED71 activity on osteoclasts

Since $1,25(OH)_2D_3$ and ED71 activities differ in osteoclasts, we utilized vitamin D receptor (VDR)-deficient mice to test whether

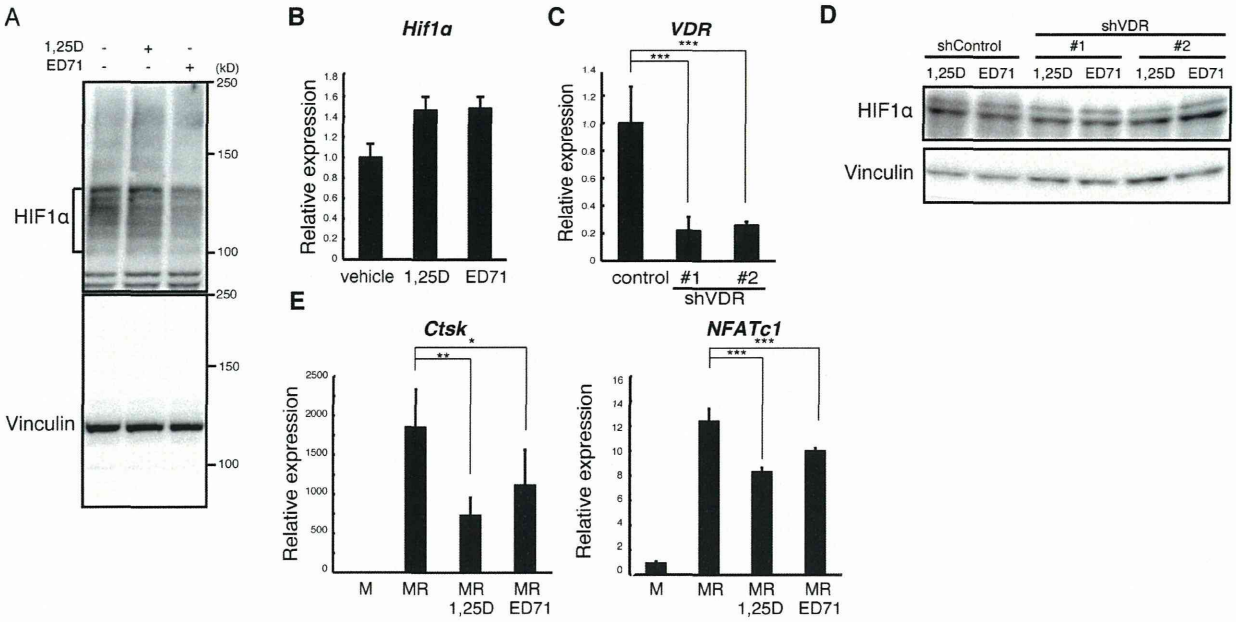

Figure 5. HIF1α protein is suppressed by ED71 but not by $1,25(OH)_2D_3$. (**A**) Western analysis of Raw264.7 cells cultured in hypoxic conditions with or without 10^{-7} M of ED71 or $1,25(OH)_2D_3$ (1,25D). (**B**) *Hif1α* mRNA levels in Raw264.7 cells cultured in hypoxic conditions were analyzed by realtime PCR in the presence or absence of 10^{-7} M ED71 or $1,25(OH)_2D_3$. Data represent mean *Hif1α* expression relative to that of *Actb* ± SD ($n=5$). (**C**) Levels of *VDR* transcripts in Raw264.7 cells transfected with shRNA targeting the VDR (shVDR) or control shRNA (Control) were determined by realtime PCR. Data represent mean *VDR* expression relative to that of *Actb* ± SD ($n=5$). (**D**) Western analysis of control (shControl) or VDR-suppressed (shVDR#1 or shVDR#2) Raw264.7 transformants cultured in hypoxic conditions with ED71 or $1,25(OH)_2D_3$ (1,25D), both at 10^{-7} M. (**E**) M-CSF-dependent Ctsk Cre/$Hif^{flox/flox}$ cells were cultured in normoxic conditions to suppress HIF1α in the presence of M-CSF (50 ng/ml) plus RANKL (25 ng/ml) with either ED71 or $1,25(OH)_2D_3$ (1,25D) both at 10^{-7}M for 4 days. Expression of *Ctsk* and *NFATc1* was then assessed by realtime PCR. Data represent mean *Ctsk* or *NFATc1* expression relative to that of *Actb* ± SD ($n=5$). *$P<0.05$; **$P<0.01$; ***$P<0.001$.
doi:10.1371/journal.pone.0111845.g005

both compounds act on osteoclasts via the VDR (Fig. 3). Osteoclast progenitors were isolated from wild-type and VDR-deficient mice and cultured in the presence of M-CSF and RANKL with or without $1,25(OH)_2D_3$ or ED71 (Fig. 3). Inhibitory effects of either $1,25(OH)_2D_3$ or ED71 on osteoclast differentiation were not seen in VDR-deficient osteoclasts (Fig. 3A and B). Similarly, inhibition of the expression of osteoclastic genes *Ctsk*, *NFATc1* and *DC-STAMP* seen following $1,25(OH)_2D_3$ or ED71 treatment was absent in osteoclasts lacking the VDR (Fig. 3C).

Moreover, decreased c-Fos protein and elevated *Ifnβ* expression seen following treatment with $1,25(OH)_2D_3$ or ED71 were abrogated in VDR-deficient osteoclasts (Fig. 4A and B), supporting the idea that both compounds act on osteoclasts via the VDR.

HIF1α is a target of ED71 but not $1,25(OH)_2D_3$ in osteoclasts

Next, we asked whether HIF1α is a target of ED71 in osteoclasts (Fig. 5). Interestingly, we found that in cultured osteoclasts, HIF1α protein levels were suppressed by ED71 but not by $1,25(OH)_2D_3$ (Fig. 5A). In contrast, *Hif1α* mRNA expression in osteoclasts was not inhibited by either treatment (Fig. 5B), suggesting that ED71 suppresses HIF1α at the protein level as demonstrated by estrogen treatment [14]. To determine if the VDR is required for ED71-mediated HIF1α protein suppression in osteoclasts, we generated two independent VDR knockdown Raw264.7 lines using shVDR#1 and shVDR#2 as well as a control (shControl) line (Fig. 5C) and then treated cells with ED71 or $1,25(OH)_2D_3$ (Fig. 5D). HIF1α protein suppression by ED71 seen in control cells was abrogated in both VDR knockdown lines, suggesting that HIF1α protein suppression by ED71 is VDR-dependent. We then isolated osteoclast progenitors from Ctsk Cre/$Hif1α^{flox/flox}$ mice, cultured them in normoxic conditions to suppress HIF1α protein, and treated cells with or without ED71 or $1,25(OH)_2D_3$ (Fig. 5E). ED71 treatment effectively inhibited osteoclast differentiation, even in HIF1α-suppressed cells, suggesting that ED71 likely targets factors other than HIF1α protein in osteoclasts (Fig. 5E). However, ED71 was less effective than $1,25(OH)_2D_3$ in inhibiting osteoclastogenesis in HIF1α-suppressed cells (Fig. 5E).

Discussion

Postmenopausal osteoporosis treatment is required to prevent disruption of daily activity or adverse outcomes due to fragile fractures. Among anti-osteoporosis agents, anti-bone resorptive or bone-forming agents include bisphosphonates, selective estrogen receptor modulator (SERM), ED71 and denosumab, or teriparaside, respectively. Strong inhibition of osteoclastic activity beyond physiological levels by bisphosphonates frequently causes adverse effects such as osteonecrosis of the jaw or severely suppressed bone turnover (SSBT) [19] [20]. Meanwhile, teriparatide treatment is limited to less than two years in order to prevent development of tumors, particularly osteosarcoma.

Recently, we showed that HIF1α protein accumulation in osteoclasts following estrogen-deficiency was accompanied by osteoclast activation and bone loss in mice [14]. Either osteoclast-specific HIF1α conditional knockout or wild-type mice administered a HIF1α inhibitor were protected from

OVX-induced osteoclast activation and bone loss. Moreover, HIF1α inhibition did not interfere with physiological osteoclast activities [14]. Thus, blocking HIF1α pharmacologically could represent an ideal treatment for postmenopausal osteoporosis, as it could target pathologically-activated osteoclasts without altering physiological osteoclastogenesis required for bone turnover. In this study, we found that both ED71, which is used as therapeutic agents for postmenopausal osteoporosis therapy, inhibits HIF1α protein expression. Indeed, patients treated with ED71 exhibit reduced osteoclastic activity and increased bone mass without adverse effects such as osteopetrosis [12], jaw osteonecrosis or SSBT, as seen in treated bisphosphonate-treated patients [19] [20].

Bone is a target tissue of vitamin D, and indeed, VDR was identified in osteoblasts [21–24]. In contrast, it is controversial whether the VDR is expressed in osteoclasts, with some authors reporting expression [25–28] and others not [21,23,29,30]. Recently, Wang et al. demonstrated that the VDR is not expressed in multi-nuclear osteoclasts using immunohistochemistry of EGTA-decalcified adult mouse bones [21]. In addition, direct effects of $1,25(OH)_2D_3$ have been demonstrated in osteoclasts and osteoclast progenitors [10] [11], and here we report that these effects are VDR-dependent (Fig. 3). Taken together, these studies suggest that extremely low levels of the VDR in osteoclasts may be sufficient to transduce vitamin D signals.

ED71 and $1,25(OH)_2D_3$ have been demonstrated to inhibit osteoclast-bone resorption activity by reducing expression of the sphigosine-1-phosphate receptor 2 (S1PR2) in circulating osteoclast precursor cells and blocking the migration of these cells to the bone surface by S1P; although differences in pharmacological action between ED71 and $1,25(OH)_2D_3$ were not demonstrated [31]. Here, we observed that, although $1,25(OH)_2D_3$ was more potent than ED71 in inhibiting osteoclastogenesis induced by M-CSF and RANKL *in vitro*, HIF1α inhibition in osteoclasts was specific to ED71. We also found that ED71 inhibited osteoclastogenesis even in HIF1α-suppressed cells, suggesting that ED71 likely targets factors other than HIF1α protein in osteoclasts. However, ED71 was less effective than $1,25(OH)_2D_3$ in inhibiting osteoclastogenesis in HIF1α-suppressed cells, which contrasts with observations seen in patients where the effect of ED71 on osteoclastogenesis is superior to that of $1,25(OH)_2D_3$ [12]. The cause of this difference remains to be elucidated, but the difference of potential activity to target HIF1α-protein in osteoclasts explains, at least in part, this difference. In addition, it is possible that ED71 inhibits osteoclastogenesis through effects on different cell types. Further investigations are needed to define molecular actions of vitamin D3 analogues on bone metabolism. Nonetheless, HIF1α inhibition could serve as an index to assess osteoclastogenesis *in vitro* when developing anti-osteoporosis agents. Moreover, our study indicates that targeting HIFα could constitute an effective treatment for osteoporosis, one that would not interfere with physiological bone turnover.

Acknowledgments

This work was supported by a grant-in-aid for Scientific Research. We thank Prof. M. Suematsu and Dr. Y.A. Minamishima for technical support in performing hypoxic culture. We also thank Dr. Shigeaki Kato for providing VDR-deficient mice.

Author Contributions

Conceived and designed the experiments: HM M. Matsumoto YT TM. Performed the experiments: YS YM SY M. Morita. Analyzed the data: HK EK AF WH TT RW KM. Contributed reagents/materials/analysis tools: TK. Wrote the paper: TM.

References

1. Report of a WHO Study Group (1994) Assessment of fracture risk and its application to screening for postmenopausal osteoporosis. World Health Organ Tech Rep Ser 10: 1–129.
2. Ettinger B, Pressman A, Sklarin P, Bauer DC, Cauley JA, et al. (1998) Associations between low levels of serum estradiol, bone density, and fractures among elderly women: the study of osteoporotic fractures. J Clin Endocrinol Metab 83: 2239–2243.
3. Sakuma M, Endo N, Hagino H, Harada A, Matsui Y, et al. (2011) Serum 25-hydroxyvitamin D status in hip and spine-fracture patients in Japan. J Orthop Sci 16: 418–423.
4. Yoshizawa T, Handa Y, Uematsu Y, Takeda S, Sekine K, et al. (1997) Mice lacking the vitamin D receptor exhibit impaired bone formation, uterine hypoplasia and growth retardation after weaning. Nat Genet 16: 391–396.
5. Winzenberg T, Jones G (2013) Vitamin D and bone health in childhood and adolescence. Calcif Tissue Int 92: 140–150.
6. Plum LA, DeLuca HF (2010) Vitamin D, disease and therapeutic opportunities. Nat Rev Drug Discov 9: 941–955.
7. Takahashi N, Akatsu T, Udagawa N, Sasaki T, Yamaguchi A, et al. (1988) Osteoblastic cells are involved in osteoclast formation. Endocrinology 123: 2600–2602.
8. Yasuda H, Shima N, Nakagawa N, Yamaguchi K, Kinosaki M, et al. (1998) Osteoclast differentiation factor is a ligand for osteoprotegerin/osteoclastogenesis-inhibitory factor and is identical to TRANCE/RANKL. Proc Natl Acad Sci U S A 95: 3597–3602.
9. Miyamoto T, Suda T (2003) Differentiation and function of osteoclasts. Keio J Med 52: 1–7.
10. Takasu H, Sugita A, Uchiyama Y, Katagiri N, Okazaki M, et al. (2006) c-Fos protein as a target of anti-osteoclastogenic action of vitamin D, and synthesis of new analogs. J Clin Invest 116: 528–535.
11. Sakai S, Takaishi H, Matsuzaki K, Kaneko H, Furukawa M, et al. (2009) 1-Alpha, 25-dihydroxy vitamin D3 inhibits osteoclastogenesis through IFN-beta-dependent NFATc1 suppression. J Bone Miner Metab 27: 643–652.
12. Matsumoto T, Ito M, Hayashi Y, Hirota T, Tanigawara Y, et al. (2011) A new active vitamin D3 analog, eldecalcitol, prevents the risk of osteoporotic fractures—a randomized, active comparator, double-blind study. Bone 49: 605–612.
13. Nelson ER, Wardell SE, McDonnell DP (2013) The molecular mechanisms underlying the pharmacological actions of estrogens, SERMs and oxysterols: implications for the treatment and prevention of osteoporosis. Bone 53: 42–50.
14. Miyauchi Y, Sato Y, Kobayashi T, Yoshida S, Mori T, et al. (2013) HIF1alpha is required for osteoclast activation by estrogen deficiency in postmenopausal osteoporosis. Proc Natl Acad Sci U S A 110: 16568–16573.
15. Yagi M, Miyamoto T, Sawatani Y, Iwamoto K, Hosogane N, et al. (2005) DC-STAMP is essential for cell-cell fusion in osteoclasts and foreign body giant cells. J Exp Med 202: 345–351.
16. Miyamoto H, Suzuki T, Miyauchi Y, Iwasaki R, Kobayashi T, et al. (2012) DC-STAMP is essential for cell-cell fusion in osteoclasts and foreign body giant cells. J Bone Miner Res 27: 1289–1297.
17. Zhao B, Takami M, Yamada A, Wang X, Koga T, et al. (2009) Interferon regulatory factor-8 regulates bone metabolism by suppressing osteoclastogenesis. Nat Med. 15: 1066–1071.
18. Nishikawa K, Nakashima T, Hayashi M, Fukunaga T, Kato S, et al. (2010) Blimp1-mediated repression of negative regulators is required for osteoclast differentiation. Proc Natl Acad Sci U S A. 107: 3117–3122.
19. Migliorati CA (2003) Bisphosphanates and oral cavity avascular bone necrosis. J Clin Oncol 21: 4253–4254.
20. Visekruna M, Wilson D, McKiernan FE (2008) Severely suppressed bone turnover and atypical skeletal fragility. J Clin Endocrinol Metab 93: 2948–2952.
21. Wang Y, Zhu J, Deluca HF (2014) Identification of the vitamin d receptor in osteoblasts and chondrocytes but not osteoclasts in mouse bone. J Bone Miner Res 29: 685–692.
22. Berger U, Wilson P, McClelland RA, Colston K, Haussler MR, et al. (1988) Immunocytochemical detection of 1,25-dihydroxyvitamin D receptors in normal human tissues. J Clin Endocrinol Metab 67: 607–613.
23. Clemens TL, Garrett KP, Zhou XY, Pike JW, Haussler MR, et al. (1988) Immunocytochemical localization of the 1,25-dihydroxyvitamin D3 receptor in target cells. Endocrinology 122: 1224–1230.
24. Narbaitz R, Stumpf WE, Sar M (1981) The role of autoradiographic and immunocytochemical techniques in the clarification of sites of metabolism and action of vitamin D. J Histochem Cytochem 29: 91–100.
25. Johnson JA, Grande JP, Roche PC, Kumar R (1996) Ontogeny of the 1,25-dihydroxyvitamin D3 receptor in fetal rat bone. J Bone Miner Res 11: 56–61.

26. Mee AP, Hoyland JA, Braidman IP, Freemont AJ, Davies M, et al. (1996) Demonstration of vitamin D receptor transcripts in actively resorbing osteoclasts in bone sections. Bone 18: 295–299.
27. Menaa C, Barsony J, Reddy SV, Cornish J, Cundy T, et al. (2000) 1,25-Dihydroxyvitamin D3 hypersensitivity of osteoclast precursors from patients with Paget's disease. J Bone Miner Res 15: 228–236.
28. Langub MC, Reinhardt TA, Horst RL, Malluche HH, Koszewski NJ (2000) Characterization of vitamin D receptor immunoreactivity in human bone cells. Bone 27: 383–387.
29. Boivin G, Mesguich P, Pike JW, Bouillon R, Meunier PJ, et al. (1987) Ultrastructural immunocytochemical localization of endogenous 1,25-dihydroxyvitamin D3 and its receptors in osteoblasts and osteocytes from neonatal mouse and rat calvaria. Bone Miner 3: 125–136.
30. Merke J, Klaus G, Hugel U, Waldherr R, Ritz E (1986) No 1,25-dihydroxyvitamin D3 receptors on osteoclasts of calcium-deficient chicken despite demonstrable receptors on circulating monocytes. J Clin Invest 77: 312–314.
31. Kikuta J, Kawamura S, Okiji F, Shirazaki M, Sakai S, et al. (2013) Sphingosine-1-phosphate-mediated osteoclast precursor monocyte migration is a critical point of control in antibone-resorptive action of active vitamin D. Proc Natl Acad Sci U S A 110: 7009–7013.

Oncogene (2014) **33,** 4236–4241

www.nature.com/onc

OPEN

ORIGINAL ARTICLE

TNFα promotes osteosarcoma progression by maintaining tumor cells in an undifferentiated state

T Mori[1,7], Y Sato[1,2,7], K Miyamoto[1,7], T Kobayashi[1,3], T Shimizu[4,5], H Kanagawa[1], E Katsuyama[1], A Fujie[1], W Hao[1], T Tando[1], R Iwasaki[6], H Kawana[6], H Morioka[1], M Matsumoto[1], H Saya[4], Y Toyama[1] and T Miyamoto[1,3]

Chronic inflammation is frequently associated with tumorigenesis in elderly people. By contrast, young people without chronic inflammation often develop tumors considered independent of chronic inflammation but driven instead by mutations. Thus, whether inflammation has a significant role in tumor progression in tumors driven by mutations remains largely unknown. Here we show that TNFα is required for the tumorigenesis of osteosarcoma, the most common tumor in children and adolescents. We show that transplantation of AX osteosarcoma cells, which harbor mutations driving c-Myc overexpression and Ink4a-deficiency, in wild-type mice promotes lethal tumorigenesis accompanied by ectopic bone formation and multiple metastases, phenotypes seen in osteosarcoma patients. Such tumorigenesis was completely abrogated in TNFα-deficient mice. AX cells have the capacity to undergo osteoblastic differentiation; however, that activity was significantly inhibited by TNFα treatment, suggesting that TNFα maintains AX cells in an undifferentiated state. TNFα inhibition of AX cell osteoblastic differentiation occurred through ERK activation, and a pharmacological TNFα inhibitor effectively inhibited both AX cell tumorigenesis and increased osteoblastic gene expression and increased survival of tumor-bearing mice. Lethal tumorigenesis of AX cells was also abrogated in IL-1α/IL-1β doubly deficient mice. We found that both TNFα and IL-1 maintained AX cells in an undifferentiated state via ERK activation. Thus, inflammatory cytokines are required to promote tumorigenesis even in mutation-induced tumors, and TNFα/IL-1 and ERK may represent therapeutic targets for osteosarcoma.

Oncogene (2014) **33,** 4236–4241; doi:10.1038/onc.2013.545; published online 16 December 2013

Keywords: osteosarcoma; tumorigenesis; osteoblast differentiation; gene-mutation; TNF α

INTRODUCTION

To date, one-third of the populations of developed countries die of malignant tumors.[1] Continuous exposure to inflammatory cytokines is known to cause tumorigenesis;[2] thus controlling chronic inflammation is crucial to prevent tumor progression, particularly in the elderly.[3] By contrast, tumors developed due to mutations are thought to be largely driven by intrinsic signals emerging from damage to tumor-initiating genes, formation of chimeric proteins due to translocation or loss of tumor suppressor genes.[4]

Osteosarcoma is a rare malignancy but the most common bone sarcoma in children and adolescents.[5] Osteosarcoma frequently metastasizes to tissues such as lung, leading to mortality.[6] As osteosarcoma develops in young people free from chronic inflammation, tumor progression has been considered independent of inflammation. Osteosarcoma originates from mesenchymal stem cells and osteoblastic cells and is defined as an 'osteoid-producing' tumor.[7] Thus, ectopic bone formation is frequently detected in osteosarcoma patients at both primary tumor sites and metastatic sites.[8] As osteoid and bones form at the terminal stage of osteoblast differentiation, osteosarcoma exhibits terminally differentiated osteoblastic phenotypes. Osteosarcoma cells also exhibit differentiation-arrested phenotypes and continuous proliferation, as seen in other malignant tumors. How both differentiated and de-differentiated phenotypes are regulated concomitantly in osteosarcoma remains largely unknown. Osteosarcoma often promotes local inflammation and is thus considered an activator of local immune responses. Indeed, several inflammatory cytokines are reportedly upregulated in the sera of osteosarcoma patients;[9] thus far, however, the roles of inflammation in osteosarcoma have not been characterized.

Development of protocols employing cytotoxic chemotherapy drugs as well as diagnostic tools such as magnetic resonance imaging have improved the prognosis and survival rate for osteosarcoma patients. Nonetheless, ~30% of osteosarcoma patients die with metastasis or tumor recurrence,[10] and the survival rate of osteosarcoma patients has not substantially improved in the last 20 years.[11] Therefore, novel targets are required to treat these patients.

Animal models are useful for the development of new chemotherapeutic agents for osteosarcoma. Historically, a spontaneous osteosarcoma animal model or a model based on exposure to a radioactive agent has been utilized.[12] However, ectopic bone formation is not evident in the spontaneous model, and only a small proportion of human osteosarcomas are radiation-induced.[13] Xenograft models using tissues from

[1]Department of Orthopedic Surgery, Keio University School of Medicine, Tokyo, Japan; [2]Department of Musculoskeletal Reconstruction and Regeneration Surgery, Keio University School of Medicine, Tokyo, Japan; [3]Department of Integrated Bone Metabolism and Immunology, Keio University School of Medicine, Tokyo, Japan; [4]Division of Gene Regulation, Institute for Advanced Medical Research, Keio University School of Medicine, Tokyo, Japan; [5]Department of Pathophysiology, School of Pharmacy and Pharmaceutical Sciences, Hoshi University, Tokyo, Japan and [6]Department of Dentistry and Oral Surgery, Keio University School of Medicine, Tokyo, Japan. Correspondence: Dr T Miyamoto, Department of Orthopedic Surgery, Keio University School of Medicine, 35 Shinano-machi, Tokyo 160-8582, Japan.
E-mail: miyamoto@z5.keio.jp
[7]These authors contributed equally to this work.
Received 29 October 2013; accepted 5 November 2013; published online 16 December 2013

osteosarocoma patients, such as MG63 cells, have also been developed but, again, ectopic bone formation has not been detected in these animals. More recently, a transplantable mouse osteosarcoma model has been developed based on the AX cell line.[14] Mesenchymal AX cells isolated from INK4a-deficient mice were transduced with c-Myc and transplanted into wild-type mice, resulting in the formation of osteosarcoma-producing osteoid and ectopic bone.[14] In wild-type mice the frequency of tumor formation and metastasis to various tissues is reportedly 100% in this model, making it a useful tool to analyze mechanisms of tumor development in a de-differentiated state accompanied by ectopic bone formation, as seen in human osteosarcoma patients.

Here we found that TNFα produced by host macrophages functions to maintain osteoarcoma cells in an undifferentiated state and is required for tumor progression. TNFα-deficient mice transplanted with AX cells exhibited completely abrogated tumor development, and pharmacological inhibition of TNFα inhibited tumor growth and elevated osteoblastic differentiation *in vivo*. Similarly, osteoblastogenesis in AX cells was significantly inhibited by IL-1 treatment, and tumor development was abrogated in IL-1α/IL-1β doubly deficient mice. Finally, we show that TNFα and IL-1 inhibited osteoblastic differentiation in AX cells through ERK activation. Thus, exogenous inflammatory cytokines are required for tumorigenesis by maintaining an undifferentiated state even in mutation-induced osteosarcoma. These findings suggest that inflammatory factors and ERKs represent potential therapeutic targets for osteosarcoma.

RESULTS

IL-6 is upregulated in osteosarcoma-bearing mice but does not function in osteosarcoma progression

We utilized the AX osteosarcoma model to establish osteosarcoma *in vivo* and analyze levels of serum cytokines and chemokines in tumor-bearing mice. Among cytokines and chemokines tested, we observed significantly high levels of IL-6, an inflammatory cytokine, in AX cell-bearing mice compared with non-tumor-bearing controls (Figure 1a). Inflammation is often seen in human

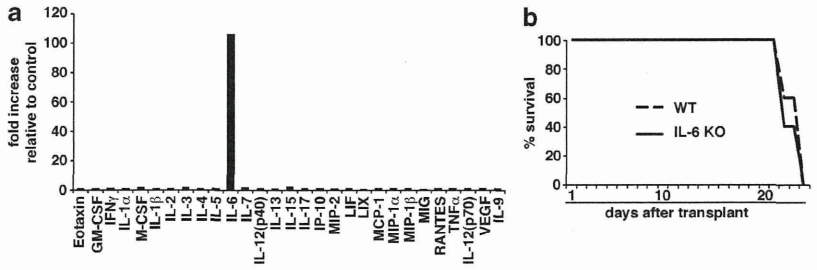

Figure 1. Serum IL-6 levels are upregulated in mice transplanted with AX cells, but IL-6 does not function in lethal AX cell progression. (**a**) AX cells were transplanted into wild-type mice intraperitoneally, and 2 weeks later serum was collected and various cytokine/chemokine levels were measured and compared with those in non-tumor-bearing mice. Data are shown as mean relative cytokine and chemokine levels in serum from AX cell-injected mice compared with those from non-tumor-bearing mice ($n=5$). (**b**) *IL-6*$^{-/-}$ mice and littermates were transplanted with AX cells intraperitoneally and their survival curves were drawn ($n=5$).

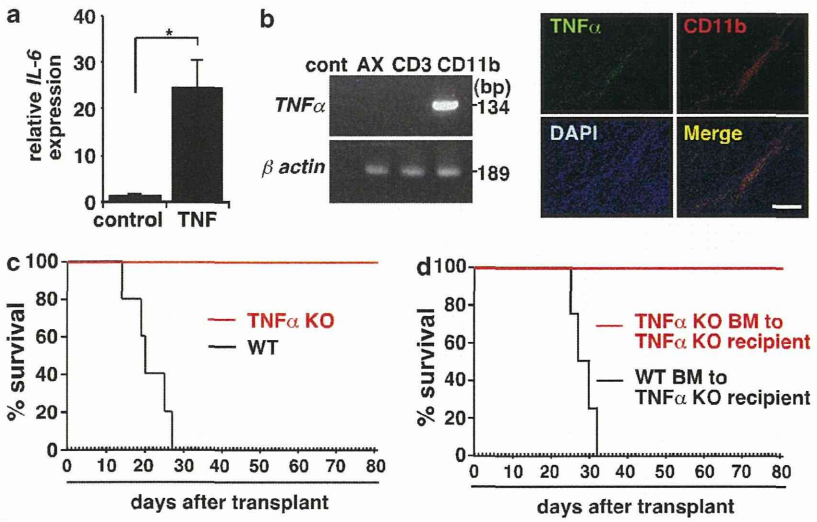

Figure 2. TNFα produced by tumor-associated macrophages is essential for AX cell lethality. (**a**) Total RNA was prepared from AX cells treated with TNFα (10 ng/ml) for 24 h, and *IL-6* expression relative to *β-actin* was analyzed by quantitative real-time PCR ($n=3$).*$P<0.01$. (**b**) Wild-type mice were transplanted with AX cells intraperitoneally. Seven days later, AX cells (EGFP$^+$ cells), CD3$^+$ T cells and CD11b$^+$ macrophages were sorted, and *TNFα* expression was analyzed by RT–PCR (left). TNFα protein expression was also analyzed by immunofluorescence staining at primary tumor sites. Paraffin sections were stained with PE-conjugated rat anti-CD11b antibody and rabbit anti-TNFα antibody followed by Alexa488-conjugated anti-rabbit Ig' antibody and observed under a fluorescent microscopy (right). Nuclei were visualized using DAPI. Bar, 100 μm. (**c**) *TNFα*$^{-/-}$ mice and wild-type littermates were transplanted with AX cells intraperitoneally and survival curves were drawn ($n=5$). (**d**) *TNFα*$^{-/-}$ mice were lethally irradiated and BM cells were reconstituted by transplantation of BM cells isolated from wild-type or *TNFα*$^{-/-}$ mice. Four months later, AX cells were transplanted into mice intraperitoneally and survival curves were drawn ($n=5$).

osteosarcoma patients,[9] and IL-6 is implicated in the development of various tumors.[15–17] Thus, we transplanted AX cells into IL-6-deficient or wild-type mice in order to compare mouse survival rates (Figure 1b). However, survival rates of AX cell-bearing mice of either genotype were comparable (Figure 1b), suggesting that IL-6 does not function in AX cell tumorigenesis *in vivo*.

TNFα produced by macrophages is required for osteosarcoma progression

Next, we analyzed signals upstream of IL-6 induction in AX cells, and found that *IL-6* mRNA level was significantly upregulated by TNFα stimulation of AX cells (Figure 2a). To assess which cells express TNFα *in vivo*, AX cells, tumor-associated CD11b-positive macrophages and CD3-positive T cells were isolated from primary tumor sites in tumor-bearing wild-type mice, and RT–PCR analysis for *TNFα* was performed. This analysis indicated that TNFα was produced by macrophages (Figure 2b). Immunohistochemical analysis confirmed TNFα expression in CD11b-positive tumor-associated macrophages (Figure 2b). When we transplanted AX cells into TNFα-deficient or wild-type mice, we found that in mice lacking TNFα, lethal tumor progression was completely abrogated *in vivo* (Figure 2c). The bone marrow (BM) of TNFα-deficient mouse was reconstructed by transplantation using wild-type or TNFα-deficient BM cells, followed by lethal irradiation, and AX cells were then transplanted into both types of mice (Figure 2d). TNFα-deficient mice transplanted with TNFα-deficient BM cells survived, whereas lethal tumor progression was seen in all mice transplanted with wild-type BM cells (Figure 2d). These data suggest that local TNFα production by macrophages is required for AX cell tumor progression, despite the fact that AX cells harbor mutations that lead to tumor development. Similarly, *IL-6* expression was significantly upregulated by IL-1β stimulation in AX cells *in vitro* (Supplementary Figure S1a), and lethal tumor progression in IL-1α and IL-1β doubly deficient mice (IL-1 DKO) transplanted with AX cells was totally abrogated compared with wild-type mice (Supplementary Figure S1b). Thus, TNFα and IL-1 promote tumor progression, which underlies mortality.

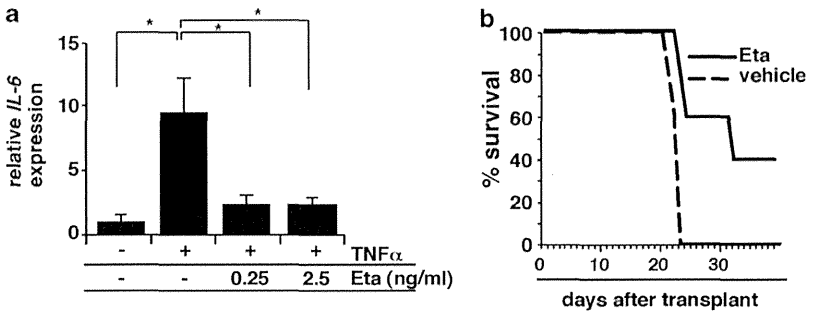

Figure 3. Etanercept improves the survival rate of AX cell-transplanted mice *in vivo*. (**a**) Total RNA was prepared from AX cells treated with TNFα (10 ng/ml) and Etanercept (Eta) (0.25 ng/ml, 2.5 ng/ml) for 24 h, and *IL-6* expression relative to *β-actin* was analyzed by quantitative real-time PCR. Data represent mean *IL-6* expression relative to *β-actin* ± s.d. ($n = 3$). *$P < 0.01$. (**b**) Wild-type mice injected with AX cells intraperitoneally at day 0 were treated with Etanercept or vehicle for 3 weeks (twice per week) from day 0, and survival curves were drawn ($n = 5$).

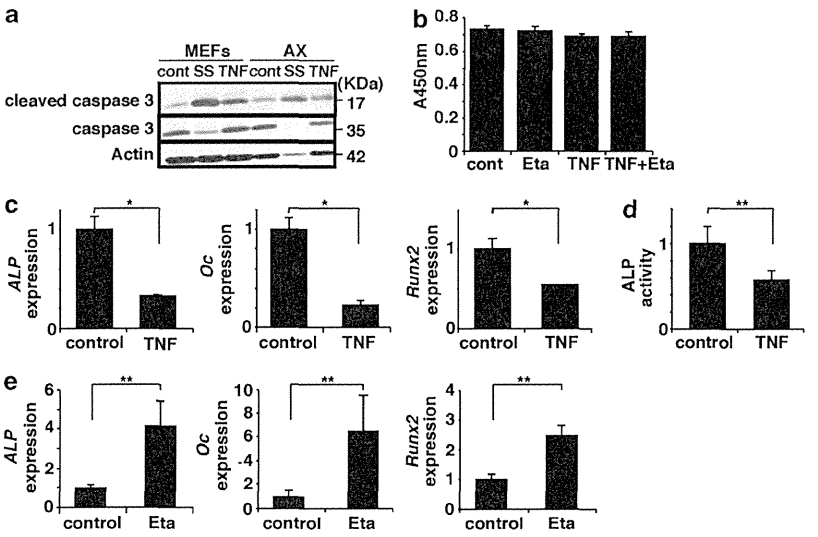

Figure 4. TNFα inhibits osteoblastic differentiation of AX cells. (**a**) Whole-cell lysates of mouse embryonic fibroblasts or AX cells stimulated with TNFα (10 ng/ml) or Staurosporine (10 μg/ml) were analyzed by immunoblotting to detect cleaved caspase 3 or caspase 3. Actin served as an internal control. (**b**) Proliferation of AX cells stimulated with TNFα (10 ng/ml), Etanercept (Eta) (2.5 ng/ml) or both was analyzed. (**c**) Total RNA was prepared from AX cells treated with or without TNFα (10ng/ml) for 24 h, and expression of *ALP*, *Osteocalcin* (*Oc*) or *Runx2* relative to *β-actin* was analyzed by quantitative real-time PCR. Data represent mean *ALP*, *Oc* or *Runx2* expression relative to *β-actin* ± s.d. ($n = 3$).*$P < 0.01$;**$P < 0.05$. (**d**) ALP activity of AX cells treated with or without TNFα (10 ng/ml) for 24 h was analyzed ($n = 3$). **$P < 0.05$. (**e**) AX cells were transplanted into wild-type mice, and mice were treated with Etanercept or vehicle. After 10 days, AX cells were sorted from primary tumor sites, total RNA was prepared and expression of *ALP*, *Oc* or *Runx2* relative to *β-actin* was analyzed by quantitative real-time PCR ($n = 3$).**$P < 0.05$.

Blocking TNFα by soluble TNFα receptor inhibits lethal tumor progression

Next, we examined the effects of pharmacological TNFα-ablation on tumor progression *in vivo* (Figure 3). Etanercept, a decoy TNFα receptor, is a soluble form of TNFα receptor and is a TNFα inhibitor utilized to treat patients with rheumatoid arthritis by subcutaneous injection.[18] The significantly upregulated *IL-6* expression seen in AX cells following TNFα stimulation was inhibited by TNFα inhibitor treatment *in vitro* (Figure 3a). We then injected TNFα inhibitor subcutaneously into AX cell-bearing wild-type mice and observed that treatment significantly increased the survival of tumor-bearing mice relative to vehicle-treated mice (Figure 3b). Thus, TNFα could serve as a target to antagonize the lethal progression of osteosarcoma.

TNFα inhibits osteoblastic differentiation of AX cells

TNFα promotes apoptosis by activating caspase 3.[19] Indeed, levels of cleaved caspase 3, the activated form of caspase 3, increased following TNFα stimulation of primary mouse embryonic fibroblasts *in vitro* (Figure 4a). In contrast, cleaved caspase 3 levels were not elevated by TNFα stimulation of AX cells (Figure 4a), suggesting that AX cells are resistant to TNFα-induced apoptosis. AX cell proliferation *in vitro* was unchanged in the presence of TNFα, TNFα inhibitor or both (Figure 4b). However, the expression of osteoblastic genes, such as *alkaline phosphatase* (*ALP*), *osteocalcin* (*Oc*) and *Runx2*, was significantly downregulated in AX cells following TNFα treatment *in vitro* (Figure 4c), as were ALP protein levels (Figure 4d). Similar to TNFα, IL-1β treatment also significantly inhibited *ALP*, *Oc* and *Runx2* expression in AX cells (Supplementary Figure S2). Furthermore, *ALP*, *Oc* and *runx2* expression in AX cells in TNFα inhibitor-treated or IL-1 DKO mice was significantly upregulated compared with AX cells in vehicle-treated mice *in vivo* (Figure 4e and Supplementary Figure S3), suggesting that TNFα and IL-1 inhibit osteoblastic differentiation and maintain osteosarcoma cells in an undifferentiated state.

TNFα inhibits osteoblastic differentiation via the ERK pathway in AX cells

The NFκB pathway is the major signaling cascade downstream of TNFα; however, NFκB inhibition did not rescue inhibited osteoblastic differentiation mediated by TNFα seen in AX cells (Figure 5a). Similarly, inhibition of p38 and JNK did not rescue inhibited osteoblastic differentiation mediated by TNFα in AX cells (Figure 5a). However, ERK inhibition by a MEK inhibitor U0126 effectively rescued inhibited osteoblastic differentiation seen in AX cells following TNFα upregulation, and expression of osteoblastic genes, such as *ALP*, *Oc* and *Runx2*, which had been inhibited by TNFα, was restored by a treatment with an ERK inhibitor *in vitro* (Figure 5a). Neither TNFα treatment, IL-1β treatment nor ERK inhibition altered AX cell proliferation (Figure 5b), suggesting that ERK is specifically required to inhibit osteoblastic differentiation rather than to activate AX cell proliferation. These results suggest that TNFα and IL-1 promote tumorigenesis by maintaining AX cells in an undifferentiated state *via* ERK activation.

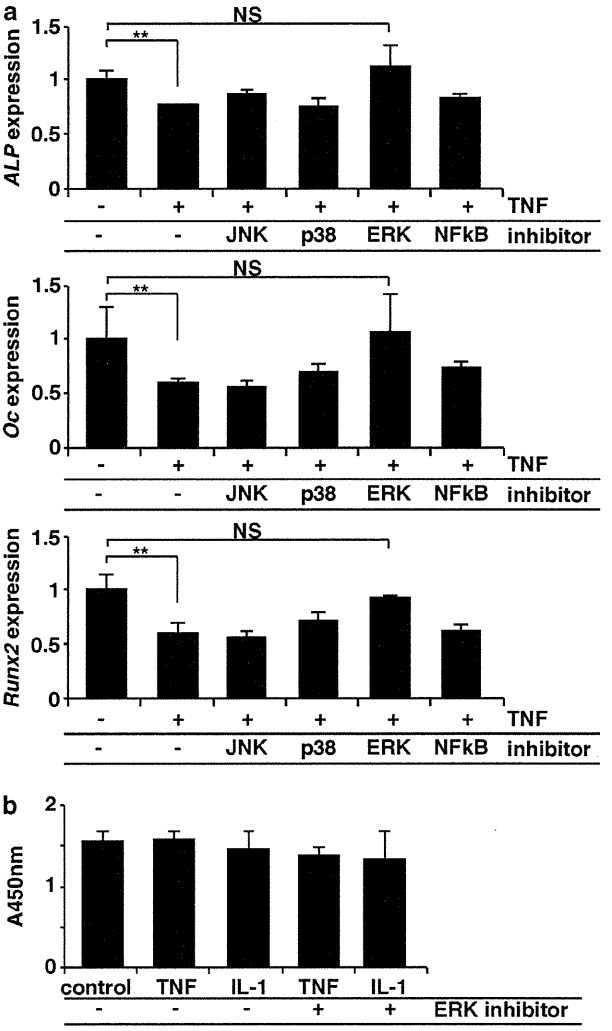

Figure 5. Inhibition of osteoblastogenesis of AX cells by TNFα is mediated by ERK. (**a**) Total RNA was prepared from AX cells treated with TNFα (10 ng/ml) in the presence or absence of the inhibitors of JNK, p38, ERK or NFκB, and expression of *ALP*, *Osteocalcin* (*Oc*) or *Runx2* relative to *β-actin* was analyzed by quantitative real-time PCR. Data represent mean *ALP*, *Oc* or *Runx2* expression relative to *β-actin* ± s.d. ($n = 3$). $^{**}P < 0.05$; NS, not significant. (**b**) Proliferation of AX cells stimulated with TNFα, IL-1β, TNFα plus an ERK inhibitor or IL-1β plus an ERK inhibitor for 24 h was analyzed ($n = 3$).

DISCUSSION

Numerous factors have been implicated in tumorigenesis, such as mutations, chronic inflammation resulting from bacterial or viral infection and prolonged exposure to radiation or oncogenic chemicals.[20] Tumors associated with mutations, chromosomal translocations or mutations in tumor suppressor genes such as breast cancer susceptibility genes 1 and 2 undergo rapid tumorigenesis,[21] and such tumors are generally considered not to require inflammatory stimuli. However, our results in an osteosarcoma model indicate that inflammation is required for tumorigenesis even in mutation-induced tumors.

AX cells are tumor cells marked by INK4a deficiency and c-Myc oncogene overexpression.[14,22–25] FGF2 produced by tumor-associating fibroblasts reportedly contributes to maintain cellular immaturity and aggressiveness.[23] Interestingly, we found that inhibition of osteoblastic differentiation by TNFα or IL-1 through ERK was required for AX cell tumorigenesis through the maintenance of an undifferentiated state. Although IL-6 is an inflammatory cytokine implicated in tumorigenesis of various cancers,[15,16] IL-6 was not required for tumor development in this osteosarcoma model. Therefore, inflammatory cytokines, such as TNFα or IL-1 or ERKs could serve as therapeutic targets for such mutation-induced tumors.

Osteosarcoma is an osteoid-producing tumor, and given that osteoid and bone matrix are produced at the terminal stage of osteoblast differentiation, osteosarcoma exhibits terminally

differentiated osteoblastic phenotypes. Osteosarcoma cells reportedly express bone morphogenic protein and form ectopic bone.[26] Nonetheless, maintenance of an undifferentiated state occurs in osteosarcoma, even under the highly differentiated condition evidenced by ectopic tumor bone formation or bone morphogenic protein expression.

Proliferation is terminated by differentiation signals in normal cells. In tumors, differentiation is disrupted or severely arrested, allowing tumors to continuously proliferate and promoting tumor progression. Thus, differentiation-inducing therapy is often effective in differentiation-arrested malignant tumors such as acute promyelocytic leukemia (PML).[27] Most PML occurs in children, driven by chromosomal translocation between chromosomes 15 and 17, which gives rise to the chimeric protein PML-RARα and induces differentiation arrest.[28] Treatment of PML patients with all-*trans* retinoic acid promotes PML cell differentiation and significantly increases survival rate.[27] In our model, differentiation arrest in osteosarcoma occurs via the TNFα/IL-1-ERK pathway. Our findings may also apply to other tumor types and contribute to the development of differentiation-inducing therapies in those malignancies. ERK signaling has diverse roles in regulating cellular proliferation and differentiation.[29] Various cytokine and growth factor signals stimulate the ERK pathway, and subsequent ERK phosphorylation transduces cellular responses to that stimulation.[30] Although ERK signaling has been implicated in inducing cellular differentiation,[31] our model demonstrates that ERK induces differentiation arrest in osteosarcoma, suggesting that responses to ERK signals are likely cell type-specific. Assessing inflammation or ERK activation in tumor biopsy samples before starting chemotherapies might implicate inflammatory cytokines or ERK as additional or alternative therapeutic targets for tumors, in addition to conventional cytotoxic chemotherapies.

Overall, our findings shed light on novel mechanisms of tumorigenesis in mutation-induced tumors and suggest a novel differentiation-inducing therapy to treat those tumors by targeting ERK and inflammatory cytokines such as TNFα and IL-1.

MATERIALS AND METHODS

Chemicals and reagents

Etanercept, a tumor necrosis factor antagonist, was purchased from Takeda Pharmaceutical Co. (Osaka, Japan). AZD6244, a MEK1 inhibitor, was purchased from Selleck Chemicals (Houston, TX, USA). Recombinant mouse IL-1β and mouse TNFα were purchased from PeproTech Ltd. (London, UK).

Cell culture and real-time PCR analysis

AX cells were established and characterized by Shimizu *et al.*,[14,22–24] and were maintained in DMEM (Sigma-Aldrich, St Louis, MO, USA) containing 10% FBS (JRH Biosciences, Kansas, TX, USA), 1% GlutaMax and antibiotics.

Total RNAs were isolated from either cultured or sorted cells using TRIzol reagent (Invitrogen, Tokyo, Japan). cDNAs were synthesized from total RNAs using oligo(dT) primer and reverse transcription (Wako Pure Chemicals Industries, Osaka, Japan). Real-time PCR was performed using SYBR Premix ExTaq II (Takara Bio Inc., Shiga, Japan) with a DICE Thermal cycler (Takara Bio Inc.), according to the manufacturer's instructions. Samples were matched to a standard curve generated by amplifying serially diluted products using the same PCR reactions. *β-actin* expression served as an internal control. Primer sequences were as follows:

β-actin forward: 5′-TGAGAGGGAAATCGTGCGTGAC-3′;
β-actin reverse: 5′-AAGAAGGAAGGCTGGAAAAGAG-3′;
IL6 forward: 5′-CAAAGCCAGAGTCCTTCAGAG-3′;
IL6 reverse: 5′-GTCCTTAGCCACTCCTTCTG-3′;
IL1alpha forward: 5′-TGCAGTCCATAACCCATGATC-3′;
IL1alpha reverse: 5′-ACAAACTTCTGCCTGACGAG-3′;
TNF alpha forward: 5′-CTTCTGTCTACTGAACTTCGGG-3′;
TNF alpha reverse: 5′-CAGGCTTGTCACTCGAATTTTG-3′;
ALP forward: 5′-ACACCTTGACTGTGGTTACTGCTGA-3′;
ALP reverse: 5′-CCTTGTAGCCAGGCCCGTTA-3′;
Osteocalcin forward: 5′-TAGCAGACACCATGAGGACCCT-3′;
Osteocalcin reverse: 5′-TGGACATGAAGGCTTTGTCAGA-3′;
Runx2 forward: 5′-GACGTGCCCAGGCGTATTTC-3′;
Runx2 reverse: 5′-AAGGTGGCTGGGTAGTGCATTC-3′.

Immunoblotting analysis

Whole-cell lysates were prepared from BM cultures using RIPA buffer (1% Triton X-100, 1% sodium deoxycholate, 0.1% SDS, 150 mM NaCl, 10 mM Tris–HCl (pH 7.5), 5 mM EDTA and a protease inhibitor cocktail; Sigma-Aldrich). Equivalent amounts of protein were separated by SDS–PAGE and transferred to a PVDF membrane (Millipore, Billerica, MA, USA). Proteins were detected using the following antibodies: anti-pERK (#9106; Cell Signaling Technology, Inc., Beverly, MA, USA), anti-ERK (#9107; Cell Signaling Technology, Inc.), cleaved caspase 3 (#9661; Cell Signaling Technology, Inc.), caspase 3 (#9665; Cell Signaling Technology, Inc.) and anti-actin (A2066; Sigma-Aldrich).

Histopathology and fluorescent immunohistochemistry

Mice were killed and the primary tumor was fixed in 10% neutral-buffered formalin, decalcified in 10% ethylenediaminetetraacetic acid (EDTA) (pH 7.4), embedded in paraffin and then cut into 4-μm sections. For each fluorescent immunohistochemistry assay, sections of 4 μm thickness were cut and subjected to microwave treatment for 5 min in 1 mM EDTA (pH 8.0) for antigen retrieval. After blocking with 0.1% BSA in 100 mM Tris–HCl (pH 7.6), 150 mM NaCl, 0.01% Tween-20 (TBST) for 20 min, sections were incubated for 1 h with rabbit anti-mouse GFP, goat anti-mouse TNFα (Santa Cruz Biotechnology, Inc., Santa Cruz, CA, USA) diluted 1:100 and rat anti-mouse FITC-CD11b (BD Biosciences, CA, USA) diluted 1:200. After washing with TBST, sections were incubated with Alexa Fluor 488-conjugated donkey anti-goat IgG (Invitrogen) diluted 1:200 and Alexa Fluor 546-conjugated rabbit anti-mouse IgG (Invitrogen) diluted 1:200. Finally, sections were mounted using Dako fluorescence mounting medium. Nuclei were stained with TOTO3 (1:750; Invitrogen). Images were acquired with a laser confocal microscope (FV1000-D, Olympus, Tokyo, Japan).

Cell proliferation assay

Cells were transferred to 96-well tissue culture plates and cultured under indicated conditions. Cell proliferation was measured using a Cell Counting kit-8 (Dojindo Molecular Technologies, Inc. Kumamoto, Japan). The OD at 450 nm was read on a Labsystems Multiscan MS (Analytical Instruments, LLC, Golden Valley, MN, USA).

Alkaline phosphatase activity assay

Cells were transferred to 96-well tissue culture plates and cultured under indicated condition. Alkaline phosphatase activity was measured by TRAP and ALP Assay Kit (Takara Bio Inc.). The OD at 405 nm was read on a Labsystems Multiscan MS (Analytical Instruments).

Animal studies

TNFα$^{-/-}$ mice were purchased from The Jackson Laboratory (Bar Harbor, ME, USA). *IL-1α*$^{-/-}$*IL-1β*$^{-/-}$ mice were provided by Professor Iwakura (Tokyo University of Science). Expression of various cytokines in mouse serum was evaluated using Milliplex MAP Cytokine/Chemokine kit (Millipore). All animals were maintained under specific pathogen-free conditions in animal facilities certified by the Keio University School of Medicine Animal Care Committee. Animal protocols were approved by that committee. A total of 2.5×10^6 AX cells were injected into mice intraperitoneally or subcutaneously and survival curves were drawn. Alternatively, subcutaneous tumors were analyzed 10 days after AX cell injection. Some mice were treated with Etanercept (5 mg/kg, twice a week, intraperitoneally) or vehicle buffer, and survival curves were drawn or subcutaneous tumors were analyzed 10 days after cell injection. Etanercept was diluted in 100 μl PBS.

Statistical analysis

Statistical analysis was performed using Student's *t*-test or one-way ANOVA, followed by a Tukey–Kramer test to determine significance between groups. In this context, significant differences were defined as $P < 0.05$.

CONFLICT OF INTEREST

The authors declare no conflict of interest.

ACKNOWLEDGEMENTS

T Miyamoto was supported by a Grant-in-aid for Scientific Research, Takeda Science Foundation, Japan.

REFERENCES

1 World Health Organization. *Ten Statistical Highlights in Global Public Health. World Health Statistics.* World Health Organization: Geneva, 2007.
2 Vendramini-Costa DB, Carvalho JE. Molecular link mechanisms between inflammation and cancer. *Curr Pharm Des* 2012; **18**: 3831–3852.
3 Vasto S, Carruba G, Lio D, Colonna-Romano G, Di Bona D, Candore G *et al.* Inflammation, ageing and cancer. *Mech Ageing Dev* 2009; **130**: 40–45.
4 Kan Z, Jaiswal BS, Stinson J, Janakiraman V, Bhatt D, Stern HM *et al.* Diverse somatic mutation patterns and pathway alterations in human cancers. *Nature* 2010; **466**: 869–873.
5 Ottaviani G, Jaffe N. The epidemiology of osteosarcoma. *Cancer Treat Res* 2009; **152**: 3–13.
6 Nakamura T, Matsumine A, Matsubara T, Asamuma K, Niimi R, Uchida A *et al.* Retrospective analysis of metastatic sarcoma patients. *Oncol Lett* 2011; **2**: 315–318.
7 Dahlin DC. Pathology of osteosarcoma. *Clin Orthop Relat Res* 1975; **111**: 23–32.
8 Kim SJ, Choi JA, Lee SH, Choi JY, Hong SH, Chung HW *et al.* Imaging findings of extrapulmonary metastases of osteosarcoma. *Clin Imaging* 2004; **28**: 291–300.
9 Rutkowski P, Kamińska J, Kowalska M, Ruka W, Steffen J. Cytokine and cytokine receptor serum levels in adult bone sarcoma patients: correlations with local tumor extent and prognosis. *J Surg Oncol* 2003; **84**: 151–159.
10 Picci P. Osteosarcoma (osteogenic sarcoma). *Orphanet J Rare Dis* 2007; **23**: 2–6.
11 Mirabello L, Troisi RJ, Savage SA. Osteosarcoma incidence and survival rates from 1973 to 2004: data from the Surveillance, Epidemiology, and End Results Program. *Cancer* 2009; **115**: 1531–1543.
12 Bensted JPM, Blackett NM, Lamerton LF. Histological and dosimetric considerations of bone tumour production with radioactive phosphorus. *Br J Radiol* 1961; **34**: 160–175.
13 Sheppard DG, Libshitz HI. Post-radiation sarcomas: a review of the clinical and imaging features in 63 cases. *Clin Radiol* 2001; **56**: 22–29.
14 Shimizu T, Ishikawa T, Sugihara E, Kuninaka S, Miyamoto T, Mabuchi Y *et al.* c-MYC overexpression with loss of Ink4a/Arf transforms bone marrow stromal cells into osteosarcoma accompanied by loss of adipogenesis. *Oncogene* 2010; **29**: 5687–5699.
15 Waldner MJ, Foersch S, Neurath MF. Interleukin-6–a key regulator of colorectal cancer development. *Int J Biol Sci* 2012; **8**: 1248–1253.
16 Hoejberg L, Bastholt L, Schmidt H. Interleukin-6 and melanoma. *Melanoma Res* 2012; **22**: 327–333.
17 Sansone P, Bromberg J. Targeting the interleukin-6/Jak/stat pathway in human malignancies. *J Clin Oncol* 2012; **30**: 1005–1014.
18 Feldmann M, Maini RN. Lasker Clinical Medical Research Award. TNF defined as a therapeutic target for rheumatoid arthritis and other autoimmune diseases. *Nat Med* 2003; **9**: 1245–1250.
19 Paroni G, Henderson C, Schneider C, Brancolini C. Caspase-2-induced apoptosis is dependent on caspase-9, but its processing during UV- or tumor necrosis factor-dependent cell death requires caspase-3. *J Biol Chem* 2001; **276**: 21907–21915.
20 Morrison WB. Inflammation and cancer: a comparative view. *J Vet Intern Med* 2012; **26**: 18–31.
21 Mavaddat N, Peock S, Frost D, Ellis S, Platte R, Fineberg E *et al.* Cancer risks for BRCA1 and BRCA2 mutation carriers: results from prospective analysis of EMBRACE. *J Natl Cancer Inst* 2013; **105**: 812–822.
22 Kubota Y, Takubo K, Shimizu T, Ohno H, Kishi K, Shibuya M *et al.* M-CSF inhibition selectively targets pathological angiogenesis and lymphangiogenesis. *J Exp Med* 2009; **206**: 1089–1102.
23 Shimizu T, Ishikawa T, Iwai S, Ueki A, Sugihara E, Onishi N *et al.* Fibroblast growth factor-2 (Fgf2) is an important factor that maintains cellular immaturity and contributes to aggressiveness of osteosarcoma. *Mol Cancer Res* 2012; **10**: 454–468.
24 Ishikawa T, Shimizu T, Ueki A, Yamaguchi SI, Onishi N, Sugihara E *et al.* Twist2 functions as a tumor suppressor in murine osteosarcoma cells. *Cancer Sci* 2013; **104**: 880–888.
25 Ueki A, Shimizu T, Masuda K, Yamaguchi SI, Ishikawa T, Sugihara E *et al.* Up-regulation of Imp3 confers *in vivo* tumorigenicity on murine osteosarcoma cells. *PLoS One* 2012; **7**: e50621.
26 Yoshikawa K, Takaoka K, Hamada H, Ono K. Clinical significance of bone morphogenetic activity in osteosarcoma. A study of 20 cases. *Cancer* 1985; **56**: 1682–1687.
27 Warrell Jr RP, Frankel SR, Miller Jr WH, Scheinberg DA, Itri LM, Hittelman WN *et al.* Differentiation therapy of acute promyelocytic leukemia with tretinoin (all-trans retinoic acid). *N Engl J Med* 1991; **324**: 1585.
28 Kakizuka A, Miller Jr WH, Umesono K, Warrell Jr RP, Frankel SR, Murty VV *et al.* Chromosomal translocation t(15;17) in human acute promyelocytic leukemia fuses RAR alpha with a novel putative transcription factor, PML. *Cell* 1991; **66**: 663–674.
29 Peyssonnaux C, Eychène A. The Raf/MEK/ERK pathway: new concepts of activation. *Biol Cell* 2001; **93**: 53–62.
30 Hagemann C, Blank JL. The ups and downs of MEK kinase interactions. *Cell Signal* 2001; **13**: 863–875.
31 Marshall CJ. Specificity of receptor tyrosine kinase signaling: transient versus sustained extracellular signal-regulated kinase activation. *Cell* 1995; **80**: 179–185.

Supplementary Information accompanies this paper on the Oncogene website (http://www.nature.com/onc)

Spine

SPINE Volume 39, Number 5, pp 394-399

DIAGNOSTICS

Prevalence, Distribution, and Morphology of Thoracic Ossification of the Posterior Longitudinal Ligament in Japanese

Results of CT-Based Cross-sectional Study

Kanji Mori, MD, PhD, Shinji Imai, MD, PhD, Toshiyuki Kasahara, MD, PhD, Kazuya Nishizawa, MD, PhD, Tomohiro Mimura, MD, PhD, and Yoshitaka Matsusue, MD, PhD

Study Design. A cross-sectional study.

Objective. To gain an insight into the prevalence, morphology, and distribution of thoracic ossification of the posterior longitudinal ligament of the spine (T-OPLL) by computed tomography (CT) and review of the literature.

Summary of Background Data. The epidemiology and cause of T-OPLL remains obscure. To date, to the best of our knowledge, there is no study that has comprehensively evaluated the thoracic spine by CT to assess the prevalence, distribution, and morphology of T-OPLL in a sufficiently large size of sample with wide distribution of age.

Methods. The participants of this study were the patients who have undergone chest CT for the examination of pulmonary diseases in our institute. The patients with previous thoracic spine surgery and younger than 15 years were excluded. Prevalence, distribution, and morphology of T-OPLL were reviewed.

Results. A total of 3013 patients (1261 females and 1752 males) with the mean age of 65 years were recruited. The CT-based evidence of T-OPLL was noted in 56 (38 females and 18 males) individuals (1.9%). Most frequently encountered type was liner type, followed by continuous cylindrical type and mixed type. Continuous waveform and beaked type were less frequently encountered. Statistical analyses revealed that T-OPLL was noted at a significantly higher rate among the females. The mean age of T-OPLL–positive males was significantly higher than that of T-OPLL–negative males. Furthermore, there was significant difference of body mass index between T-OPLL–positive and T-OPLL–negative individuals. Most of T-OPLLs were confirmed in higher or middle thoracic regions and the highest peak was found at T3–T4. T-OPLL was noted after the age of 40 years with the peak distribution found at the age of 60 years.

Conclusion. The prevalence of T-OPLL in Japanese was 1.9%. Further studies that characterize definitive subtypes of T-OPLL on CT are warranted so as to establish possible association between clinical manifestations and size and/or subtypes of T-OPLL.

Key words: OPLL, computed tomography, ossification, posterior longitudinal ligament of the spine, thoracic spine, prevalence, epidemiology, morphology, classification, body mass index.

Level of Evidence: N/A

Spine 2014;39:394–399

Ossification of the posterior longitudinal ligament of the spine (OPLL), first described by Key in 1838,[1] is characterized by the heterotopic bone formation in the posterior longitudinal ligament of the spine. In 1960, Tsukimoto[2] reported first autopsy case of chronic cervical myelopathy caused by extensive cervical OPLL (C-OPLL). OPLL can result in neurological compromises through compression of spinal cord.[3]

OPLL has been assumed to occur predominantly in the East Asian population, particularly in Japanese.[4] The cervical spine is commonly affected by the OPLL,[4] thoracic OPLL (T-OPLL) is a rare but clinically significant spinal disorder that causes progressive thoracic myelopathy and it still remains one of the most challenging diseases in spine surgery.

The recent genetic analyses have led to increasing interests in understanding the underlying mechanism of ossifying plaques in OPLL.[5] In turn, several clinical reports of T-OPLL have dealt with surgical techniques and their results.[6–8] However, less attention has been paid to epidemiological aspects of this entity. The prevalence of C-OPLL in the Japanese population was reported to be 1.9% to 4.3% among people older than 30 years[9]; however that of T-OPLL has not been adequately addressed.

From the Department of Orthopaedic Surgery, Shiga University of Medical Science, Tsukinowa-cho, Seta, Otsu, Shiga, Japan.

Acknowledgment date: September 12, 2013. Revision date: November 11, 2013. Acceptance date: November 18, 2013.

The manuscript submitted does not contain information about medical device(s)/drug(s).

Health and Labour Science Research Grants funds were received in support of this work.

No other financial associations that may be relevant or seen as relevant to the submitted manuscript.

Address correspondence and reprint requests to Kanji Mori, MD, PhD, Department of Orthopaedic Surgery, Shiga University of Medical Science, Tsukinowa-cho, Seta, Otsu, Shiga, 520-2192, Japan; E-mail: kanchi@belle.shiga-med.ac.jp

DOI: 10.1097/BRS.0000000000000153

Standard plain radiograph is not an adequate modality for diagnosis of T-OPLL because of the complex anatomy of thoracic region. The radiographical evidence of T-OPLL can be masked by superimposed bony structures such as ribs.[10] In contrast, computed tomography (CT), probably the most suitable modality to identify the ossification, allows us precise localization of T-OPLL, no matter what superimposition of the thoracic complexities.[11] Recently, we have reported the epidemiological study of thoracic ossification of ligamentum flavum (T-OLF) using chest CT data over 3000 cases.[12] In this study, using same cohort, we carefully evaluated prevalence, morphology, and distribution of T-OPLL and reviewed previously published literature.

To date, to the best of our knowledge, this study encompasses the largest sample of thoracic spine studied by CT scan with wide age distribution.

MATERIALS AND METHODS

This study was performed along with the previously published study by the same author.[12]

Participants

The participants of this study were the patients who have undergone chest CT scanning for the examination of pulmonary diseases (pneumonia or pulmonary cancer and their suspicious) in our institute from January 2010 to September 2010. A total of 3013 consecutive patients were recruited for the analysis. Of the 3013 patients, 1261 were females and 1752 were males with the mean age of 65 years (range, 16–97 yr). The patients with previous thoracic spine surgery and younger than 15 years were excluded from the study. The presences of OPLL as well as clinical parameters such as age, sex, and body mass index (BMI) were retrospectively reviewed. The local ethics committee approved this study.

Radiological Examination

All chest CT scans were axial, 0.5-mm thick, sequential, and obtained in supine position without gantry tilt (120 kV, 160 mA, 0.5 s) using a Toshiba Aquilion CX (Toshiba Medical Systems Corporation, Japan). These data were reconstructed in the condition suitable for bone evaluation by the software application (AquariusNet Viewer; TeraRecon, Inc., Foster City, CA). This software application allows us to reconstruct optimal sagittal, coronal, and axial views to identify OPLL. On CT scans, lesions of OPLL are seen as ossified masses arising from posterior aspect of the vertebra.

Definitive OPLL was determined according to the previous report with slight modifications. Briefly, a positive case of OPLL was defined as the ossification, at least, thicker than 3 mm within the posterior longitudinal ligament of the spine. OPLL of hard disc type that localizes exclusively at the intervertebral disc level was not included. All CT scans were evaluated by 2 of the authors (K.M. and T.K.); differences were settled by consensus to minimize intra- and interobserver bias and errors.

To the best of our knowledge, there is no universally approved classification of T-OPLL on CT. We therefore classified T-OPLL into the following 5 subtypes; linear, beaked, continuous waveform, continuous cylindrical, or mixed type (composed of at least 2 of the first 4 types) according to the previous report[13] using sagittal reconstruction images (Figure 1). We also evaluated the number of level involved by T-OPLLs using sagittal reconstruction images. Ossification of intervertebral level such as beaked type ossification has a critical impact on the clinical results of T-OPLL[8]; the number of level involved by T-OPLL was evaluated at both vertebral and intervertebral level, yielding the minimum ossification sites of 2 and the maximum sites of 23. In turn, at the level of the largest ossification on axial image, we classified T-OPLL into 2 subtypes, that is, central and lateral deviated type, according to Matsunaga criteria.[14]

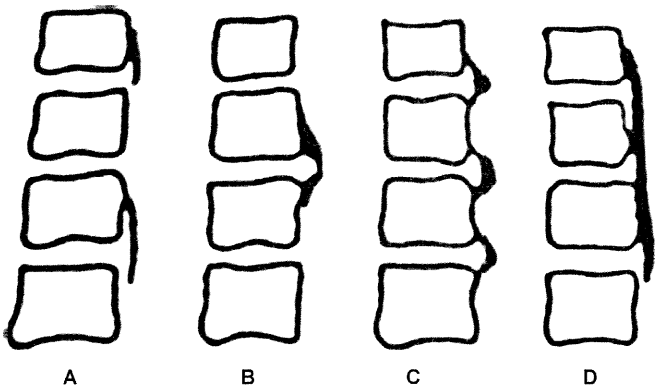

Figure 1. Classification of thoracic ossification of the longitudinal ligament.[13] **A**, Linear type. **B**, Beaked type. **C**, Continuous waveform type. **D**, continuous cylindrical type. Mixed type is defined as a combination of 2 or more different types.

Statistical Analysis

Student t test, Welch test and χ^2 test were used when appropriate. $P < 0.05$ was considered as statistically significant. The software application used for the analysis was Stata/MP 12.0 (StataCorp LP, College Station, TX).

RESULTS

Distribution and Prevalence of T-OPLLs

The CT-based evidence of T-OPLL was noted in 56 (38 females and 18 males) individuals (1.9%), and their mean age was 68 years (range, 41–88 yr; Table 1). Among T-OPLL–positive individuals, minimum and maximum number of ossification sites was 2 and 12, respectively.

Statistical analyses revealed that T-OPLL was noted at a significantly higher rate among the females ($P < 0.0001$). In addition, they also revealed that the mean age of T-OPLL–positive males was significantly higher than that of T-OPLL–negative males, 74 and 66 for the T-OPLL–positive and T-OPLL–negative males, respectively, ($P = 0.0004$; Table 1). In turn, there was no difference in the mean age between the T-OPLL–positive and T-OPLL–negative females, 64 *versus* 64, respectively ($P = 0.75$; Table 1). Furthermore, there was significant difference of BMI between T-OPLL–positive and T-OPLL–negative individuals (mean; 24 *vs.* 22, $P = 0.0076$; Table 1).

TABLE 1. Characterization of OPLL-Positive and OPLL-Negative Individuals

	OPLL					
	Male		Female		Total	
	+	−	+	−	+	−
Number	18	1734	38	1223	56	2957
Age (mean ± SD), yr	74 ± 8.3	66 ± 14	64 ± 10	64 ± 15	68 ± 11	65 ± 14
p	0.0004		0.75		0.083	
BMI (mean ± SD), kg/m²	24 ± 3.0	22 ± 3.4	23 ± 4.2	22 ± 3.6	24 ± 3.9	22 ± 3.5
P	0.013		0.059		0.0076	

Age and BMI were presented as mean ± SD.
OPLL indicates ossification of the posterior longitudinal ligament of spine; BMI, body mass index; SD, standard deviation.

Distribution of the OPLL in the thoracic segments was shown in Figure 2. Most of T-OPLLs were confirmed in higher or middle thoracic regions and the highest peak was found at T3–T4 (Figure 2). Lower thoracic region was less frequently involved. We then compared the prevalence of T-OPLL among each 10-year age group, that is, 10, 20, 30 years, and so on. T-OPLL was noted after the age of 40 years with the peak distribution found at the age of 60 years (Figure 3).

The distribution of different type of ossification was summarized in Table 2. Most frequently encountered type was liner type, followed by continuous cylindrical type and mixed type. Continuous waveform and beaked type were less frequently encountered. In turn, central involvement was observed in 42 cases, whereas lateral deviated involvement was observed in 14 cases. Large T-OPLL extended more than 50% of the anteroposterior diameter of the spinal canal was not observed.

Twelve cases (67%) of the T-OPLL–positive males and 23 cases (61%) of the T-OPLL–positive females had concomitant T-OLF.

DISCUSSION

This study disclosed the precise prevalence of T-OPLL in Japanese population. According to our review of the literature, this study is the first report of CT-based prevalence of T-OPLL.

One must acknowledge that previous epidemiological studies with less number of participants and/or limited population have hampered our knowledge. The number of epidemiological reports on the T-OPLL is much smaller than that on the C-OPLL.[15] Previously documented prevalence of T-OPLL has been roughly estimated by the instances of thoracic myelopathy as well as by surveys concomitant with that of C-OPLL.[16,17] Tsuchiya *et al*[16] reported that T-OPLL was found in 12 (16.4%) of 73 cases of C-OPLL. In turn, the report by the Japanese Ministry of Health and Welfare[18] has documented 204 cases of T-OPLL (18%) of 1157 outpatients of Orthopedic Surgery, in a multicenter study.

There have been only few studies reporting the prevalence of T-OPLL based on a survey of the general population. Through a review of literature including those written in Japanese, we encountered only 2 studies reporting the prevalence of T-OPLL[15,19] (Table 3). Ono *et al*[19] evaluated 8610 sheets of the lateral chest radiograph that were obtained as a part of physical examination of atomic bomb survivors older than 30 in Hiroshima and Nagasaki, and reported a prevalence of 0.25% in males and 0.74% in females, respectively (total prevalence: 0.56%). In turn, Ohtsuka *et al*[15] reported

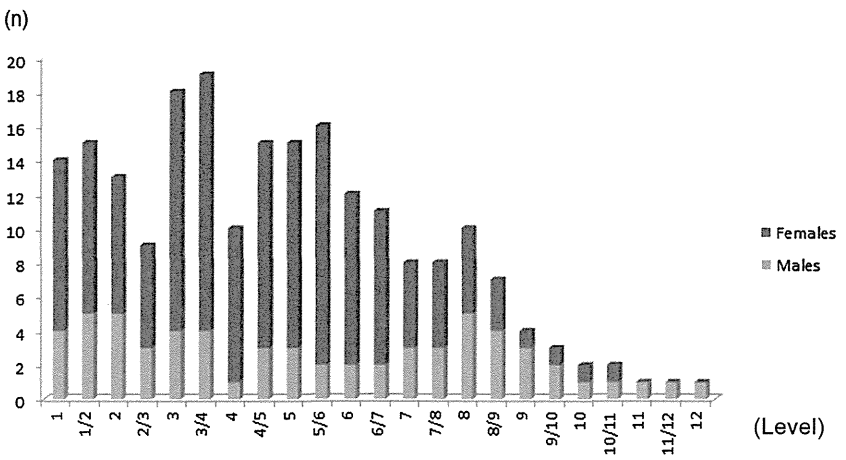

Figure 2. The distribution of T-OPLLs. T-OPLL predominantly localized higher thoracic regions and the highest peak was found at T3–T4. T-OPLL indicates thoracic ossification of the posterior longitudinal ligament.

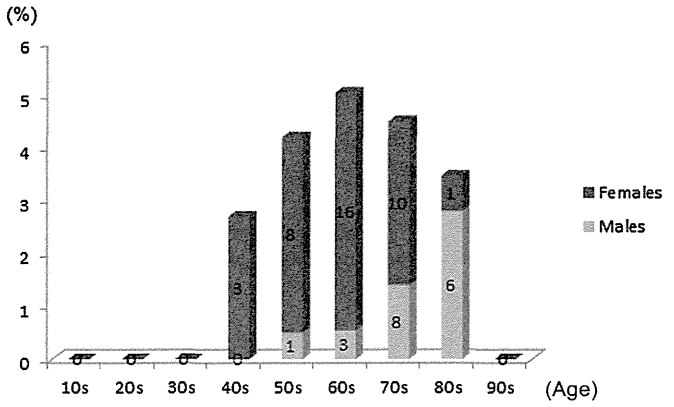

Figure 3. The age-oriented prevalence of thoracic ossification of the posterior longitudinal ligament. The figure indicates the number of the individuals.

TABLE 2. Distribution of Ossification Type of T-OPLL–Positive Individuals

Type of ossification	No. of T-OPLL–Positive Individuals (n)		
	Male	Female	Total
Linear	7	14	21
Beaked	3	3	6
Continuous waveform	2	5	7
Continuous cylindrical	2	10	12
Mixed	4	6	10

Mixed type is defined as a combination of 2 or more different types.
T-OPLL indicates thoracic ossification of the posterior longitudinal ligament of spine.

a prevalence of 0.9% in males and 0.6% in females (total prevalence: 0.8%) among 1058 general population using standard lateral thoracic spine radiographs. On the basis of these reports, Ohtsuka *et al*[15] concluded that the prevalence of T-OPLL in Japanese is below 1%, which is about one-third of the prevalence of C-OPLL.

This study revealed that the prevalence of T-OPLL is 1.0% in males and 3.0% in females (total 1.9%). Consistent with previous reports,[18,20] significant female preponderance of T-OPLL was confirmed. As we[12] and others[21,22] observed in the research for the prevalence of T-OLF by CT, higher detection rate by CT scan might have contributed to the higher prevalence of T-OPLL in this study.

It has been reported that the most frequently involved thoracic site by OPLL is T6.[15,16,18,20,23] However, our study revealed that the most frequently involved thoracic site by OPLL is more cranial level, T3–T4. Because previous studies have used standard radiographs, T-OPLL localized higher thoracic regions might have been masked by the superimposed bony structures such as shoulder and ribs. These results suggest that the diagnostic modality has an important impact on the evaluation of OPLL in thoracic region.

In previous reports, localization of T-OPLL was counted only at the level of vertebrae.[15,16,18,20,23] However, in thoracic region, ossifications of intervertebral disc levels such as beaked type ossification have critical impacts on the clinical feature.[8] We therefore considered that it is very important to evaluate the ossifications not only at the level of vertebrae but also at the level of intervertebral discs. To the best of our knowledge, there have been no epidemiological reports that focused on the ossifications at intervertebral disc levels (Figure 2).

As for the prevalence of C-OPLL among Caucasians, several previous studies have reported lower prevalence than that of the Japanese.[24,25] In turn, we could find only 1 study that reported the prevalence of T-OPLL among non-Japanese population.[26] In this report conducted in Italy, T-OPLL was confirmed in 2 cases (0.41%) among 488 adult outpatients studied from 1977 to 1983 at the Rizzoli Orthopaedic Institute, Bologna, Italy.[26] However, the prevalence of both C- and T-OPLL in the study was much higher than those of other non-Japanese reports, which has been assumed to comparable with those of Japanese. The population of this study was outpatients of Orthopaedic Surgery; it is therefore likely that selection bias of population yielded this higher prevalence of OPLL.

Since the publishing of the classical report on the pathophysiological association between OPLL and diffuse idiopathic skeletal hyperostosis (DISH),[27,28] OPLL has become increasingly recognized as an important entity occurring not only in Japanese but also in Caucasian. Further epidemiological studies are advocated to determine the accurate prevalence of OPLL among non-Japanese population.

Since the first description of OPLL,[1] pathophysiology of OPLL has remained yet undetermined over 175 years. Currently, it is assumed to be a multifactorial disease, in which environmental and genetic factors complexly interact.[29] Hypothetical contribution of genetic factors,[9,30] sex,[18] diabetes mellitus,[18,31] obesity,[31] trauma,[32] hormonal imbalance,[33] and dietary habits[29,33] have been proposed. Consistent with these reports, we confirmed significant association between sex (female preponderance), obesity (high BMI), and T-OPLL. This study confirmed that the peak prevalence of T-OPLL is noted at the age of 60 years, whereas no T-OPLL was observed in patients younger than 40 years. This finding also supports degenerative features of OPLL. It also remains unknown why unique ossification such as beaked type OPLL arises at the intervertebral disc level in thoracic region. Further examination to elucidate pathogenesis of OPLL is warranted.

Since the publication of the classical report on the association between OPLL and DISH,[27,28] OPLL has been often noticed to occur concomitant with other ossification of the spinal ligaments such as ligamentum flavum.[34] Takeuchi *et al*[35] reported case series of thoracic paraplegia due to neglected thoracic lesions developing after lumbar decompression surgery. Taking these findings into consideration; we advocate thorough evaluation of whole spine not to overlook latent risk of concomitant OPLL and OLF when treating the patients with ossification of the spinal ligaments.

TABLE 3. Previously Reported Prevalence of Ossification of the Posterior Longitudinal Ligament of the Thoracic Spine

Authors/Reported Year	Country	Sample Size	Target	Mean Age (Range), yr	Modality	Prevalence, %
Ono *et al*[19] (1982)	Japan	8610	GP	NA (<30)	Lateral chest radiographs	Males: 0.25, females: 0.74, total: 0.56
Ohtsuka *et al*[15] (1986)	Japan	1058	GP	62.8 (50–<80)	Lateral thoracic spine radiographs	Males: 0.9, females: 0.6
Mori *et al* (this study)	Japan	3013	P	65 (16–97)	Chest CT*	Males: 1.0, females: 3.0, total: 1.9

**The data were reconstructed in the condition suitable for bone evaluation by the software application.*

GP indicates general population; P, patients who have undergone chest CT scanning for the examination of pulmonary diseases; NA, not available; CT, computed tomography; MRI, magnetic resonance imaging.

Otherwise, this study imposes several limitations. This study is a patient-based study, but not a population-based study. We employed the data of chest CT examination for pulmonary diseases (pneumonia and pulmonary cancer and their suspicious) but not for general population. This is the inescapable limitation of this study. However, the favorable aspect of this study protocol is that it does not impose further radiological exposure on the participants.

We could not find the patients with systemic inflammatory/autoimmune diseases that might cause spinal manifestations in this cohort. Despite a thorough review of literature, there have been no previous studies addressing relationship between OPLL and pulmonary diseases. Nonetheless, it does not totally cancel the possibility that pulmonary diseases have no impact on the prevalence of OPLL. Possible association between OPLL and pulmonary diseases remains to be elucidated, perhaps by other studies.

In addition, it is possible that the prevalence of severe T-OPLL may be underestimated, because the patients with severe T-OPLL with neurological compromise would have visited hospital for gait disturbance not for pulmonary diseases. Indeed, no large T-OPLL, that is, ossification larger than 50% of the anteroposterior diameter of the spinal canal, was observed in this study. Accordingly, real prevalence of T-OPLL among the general population may be higher than it was calculated by the present settings.

Another limitation of this study is that we could not establish definitive subtypes of T-OPLL on CT. Furthermore, we could not evaluate clinical manifestations and OPLL observed in this study. Matsunaga *et al*[14] reported that more than 60% spinal canal stenosis by OPLL and lateral deviated type OPLL on CT were radiographical risk factors for development of cervical myelopathy.

CONCLUSION

The CT-based prevalence of T-OPLL in Japanese was 1.9%. Further studies that characterize definitive subtypes of T-OPLL on CT are warranted so as to establish possible association between clinical manifestations and size and/or subtypes of T-OPLL.

➢ Key Points

- ❑ To date, this study is the first report of CT-based prevalence of T-OPLL.
- ❑ The prevalence of T-OPLL in Japanese was 1.9% and it is more frequent in females.
- ❑ We confirmed significant association between sex (female preponderance), obesity (high BMI), and T-OPLL.
- ❑ We advocate thorough evaluation of whole spine not to overlook latent risk of concomitant OPLL and OLF when treating the patients with spinal ossification.

References

1. Key GA. On paraplegia depending on the ligament of the spine. *Guy Hosp Rep* 1838;3:17–34.
2. Tsukimoto H. A care-report autopsy of syndrome of compression of spinal cord owing to ossification within spinal canal of cervical spines. *Arch Jap Chir* 1960;29:1003–7.
3. Miyasaka K, Kaneda K, Sato S, et al. Myelopathy due to ossification or calcification of the ligamentum flavum: radiologic and histologic evaluations. *AJNR Am J Neuroradiol* 1983;4:629–32.
4. Matsunaga S, Sakou T. Epidemiology of ossification of the posterior longitudinal ligament. In: Yonenobu K, Sakou T, Ono K, eds. *OPLL, Ossification of the Longitudinal Ligament*. Tokyo, Japan: Springer-Verlag; 1997:3–17.
5. Liu Y, Zhao Y, Chen Y, et al. RUNX2 polymorphisms associated with OPLL and OLF in the Han population. *Clin Orthop Relat Res* 2010;468:3333–41.
6. Matsumoto M, Toyama Y, Chikuda H, et al. Outcomes of fusion surgery for ossification of the posterior longitudinal ligament of the thoracic spine: a multicenter retrospective survey: clinical article. *J Neurosurg Spine* 2011;15:380–5.
7. Matsumoto M, Chiba K, Toyama Y, et al. Surgical results and related factors for ossification of posterior longitudinal ligament of the thoracic spine: a multi-institutional retrospective study. *Spine* 2008;33:1034–41.
8. Matsuyama Y, Yoshihara H, Tsuji T, et al. Surgical outcome of ossification of the posterior longitudinal ligament (OPLL) of the thoracic spine: implication of the type of ossification and surgical options. *J Spinal Disord Tech* 2005;18:492–7.
9. Matsunaga S, Sakou T. Ossification of the posterior longitudinal ligament of the cervical spine: etiology and natural history. *Spine* 2012;37:E309–14.

10. Okada G, Hosoi S, Kato K, et al. Case report 779. Carbonate apatite calcification of ligamentum flavum. *Skeletal Radiol* 1993;22:211–3.
11. Li F, Chen Q, Xu K. Surgical treatment of 40 patients with thoracic ossification of the ligamentum flavum. *J Neurosurg Spine* 2006;4:191–7.
12. Mori K, Kasahara T, Mimura T, et al. Prevalence, distribution, and morphology of thoracic ossification of the yellow ligament in Japanese: results of CT-based cross-sectional study. *Spine* 2013;38:E1216–22.
13. Sakou T, Hirabayashi K. *Modified Criteria of Patient Selection for Treatment of Ossification of Spinal Ligaments. Annual Report of Task Force of Research for Ossification of Spinal Ligaments Sponsored by the Japanese Ministry of Health and Welfare* (in Japanese). 1994;11–4.
14. Matsunaga S, Nakamura K, Seichi A, et al. Radiographic predictors for the development of myelopathy in patients with ossification of the posterior longitudinal ligament: a multicenter cohort study. *Spine* 2008;33:2648–50.
15. Ohtsuka K, Terayama K, Yanagihara M, et al. An epidemiological survey on ossification of ligaments in the cervical and thoracic spine in individuals over 50 years of age. *Nihon Seikeigeka Gakkai Zasshi* 1986;60:1087–98.
16. Tsuchiya A, Imai K, Yamanouchi T, et al. Ossification of the posterior longitudinal ligament in the thoracic spine (in Japanese). *Seikeigeka* 1975;26:667–72.
17. Onji Y, Akiyama H, Shimomura Y, et al. Posterior paravertebral ossification causing cervical myelopathy. A report of eighteen cases. *J Bone Joint Surg Am* 1967;49:1314–28.
18. Tsuyama N, Kurokawa T. Ossification of the posterior longitudinal ligament in the thoracic and lumbar spine. Statistical report of ossification of the posterior longitudinal ligament for all of Japan (in Japanese). *Rinsho Seikei Geka* 1977;12:337–9.
19. Ono M, Russell WJ, Kudo S, et al. Ossification of the thoracic posterior longitudinal ligament in a fixed population. Radiological and neurological manifestations. *Radiology* 1982;143:469–74.
20. Imai T, Kakunan Y, Nakahara S, et al. Clinical study of ossification of the posterior longitudinal ligament of the thoracic spine (in Japanese). *Rinsho Seikei Geka* 1977;12:340–4.
21. Williams DM, Gabrielsen TO, Latack JT, et al. Ossification in the cephalic attachment of the ligamentum flavum. An anatomical and CT study. *Radiology* 1984;150:423–6.
22. Al-Orainy IA, Kolawole T. Ossification of the ligament flavum. *Eur J Radiol* 1998;29:76–82.
23. Akiyama N, Onari K, Kitao S, et al. Ossification of the posterior longitudinal ligament of the thoracic spine; radiological study (in Japanese). *Seikeigeka* 1981;32:1029–39.
24. Izawa K. Comparative roentgenographical study on the incidence of ossification of the posterior longitudinal ligament and other degenerative changes of the cervical spine among Japanese, Koreans, Americans, and Germans (in Japanese). *Nihon Seikeigeka Gakkai Zasshi* 1980;54:461–74.
25. Firooznia H, Benjamin VM, Pinto RS, et al. Calcification and ossification of posterior longitudinal ligament of spine: its role in secondary narrowing of spinal canal and cord compression. *N Y State J Med* 1982;82:1193–8.
26. Terayama K, Ohtsuka K. Ossification of the spinal ligament. A radiological reevaluation in Bologna, Italy. *J Jpn Orthop Assoc* 1987;61:1373–8.
27. Resnick D, Guerra J, Jr, Robinson CA, et al. Association of diffuse idiopathic skeletal hyperostosis (DISH) and calcification and ossification of the posterior longitudinal ligament. *AJR Am J Roentgenol* 1978;131:1049–53.
28. McAfee PC, Regan JJ, Bohlman HH. Cervical cord compression from ossification of the posterior longitudinal ligament in non-Orientals. *J Bone Joint Surg Br* 1987;69:569–75.
29. Okamoto K, Kobashi G, Washio M, et al. Dietary habits and risk of ossification of the posterior longitudinal ligaments of the spine (OPLL); findings from a case-control study in Japan. *J Bone Miner Metab* 2004;22:612–7.
30. Horikoshi T, Maeda K, Kawaguchi Y, et al. A large-scale genetic association study of ossification of the posterior longitudinal ligament of the spine. *Hum Genet* 2006;119:611–6.
31. Kobashi G, Washio M, Okamoto K, et al. High body mass index after age 20 and diabetes mellitus are independent risk factors for ossification of the posterior longitudinal ligament of the spine in Japanese subjects: a case-control study in multiple hospitals. *Spine* 2004;29:1006–10.
32. Katoh S, Ikata T, Hirai N, et al. Influence of minor trauma to the neck on the neurological outcome in patients with ossification of the posterior longitudinal ligament (OPLL) of the cervical spine. *Paraplegia* 1995;33:330–3.
33. Musha Y. Etiological study of spinal ligament ossification with special reference to dietary habits and serum sex hormones. *Nihon Seikeigeka Gakkai Zasshi* 1990;64:1059–71.
34. Tomita K, Kawahara N, Baba H, et al. Circumspinal decompression for thoracic myelopathy due to combined ossification of the posterior longitudinal ligament and ligamentum flavum. *Spine* 1990;15:1114–20.
35. Takeuchi A, Miyamoto K, Hosoe H, et al. Thoracic paraplegia due to missed thoracic compressive lesions after lumbar spinal decompression surgery. Report of three cases. *J Neurosurg* 2004;100(suppl 1, *Spine*):71–4.

J Orthop Sci
DOI 10.1007/s00776-014-0631-2

CASE REPORT

Cervical myelopathy due to calcification of the posterior atlantoaxial membrane associated with generalized articular deposition of calcium pyrophosphate dihydrate: a case report and review of the literature

Kanji Mori · Shinji Imai · Kazuya Nishizawa · Yoshitaka Matsusue

Received: 17 March 2014 / Accepted: 30 July 2014

Introduction

The ligamentum flavum can undergo either calcification or ossification that can lead to radiculomyelopathy [1, 2]. Calcification of the ligamentum flavum (CLF) characteristically occurs in the cervical spine in elderly women [1]. Theoretically speaking, calcification of the spinal ligament can affect any level of the cervical spine; however, we seldom encounter calcification of the posterior atlantoaxial membrane.

In the present report, we illustrate a unique case of cervical myelopathy due to calcification of the posterior atlantoaxial membrane that occurred concomitantly with generalized deposition of calcium pyrophosphate dihydrate (CPPD) as well as cervical ossification of the longitudinal ligament of the spine (OPLL).

Report of case

An 83-year-old woman visited our institution due to spastic gait, clumsiness, and numbness of bilateral hands progressing over the course of 2 months without preceding craniocervical trauma. Neurological examination revealed hyperreflexia of all four extremities, disturbance of discrete movement of bilateral hands, and bilateral positive Babinski signs. There was no bowel or bladder dysfunction. She had a history of surgical treatment of bilateral carpal tunnel release and right total knee arthroplasty. Routine blood tests were unremarkable except for a mildly increased blood sugar level (mild diabetes mellitus).

K. Mori (✉) · S. Imai · K. Nishizawa · Y. Matsusue
Department of Orthopaedic Surgery, Shiga University of Medical Science, Tsukinowa-cho, Seta, Otsu, Shiga 520-2192, Japan
e-mail: kanchi@belle.shiga-med.ac.jp

On X-ray examination, mixed-type OPLL extending from C2 to C5, retro-odontoid calcification, as well as a round calcified mass between the posterior arch of C1 and the lamina of C2 were noted (Fig. 1a). Calcified lesions were also found in the left knee, shoulders, and fingers (Fig. 1b–d). Joint fluid analyses of the left knee joint by polarization microscopy revealed CPPD crystals. Computed tomography (CT) clearly demonstrated oval calcification of the posterior atlantoaxial membrane, retro-odontoid calcification, as well as OPLL extending from C2 to C5. A calcified lesion was visualized as vague spotty images on CT (Fig. 2a, b). Subsequent magnetic resonance (MR) imaging demonstrated overt compression of the spinal cord due to calcification of the posterior atlantoaxial membrane, which was low intensity on both T1- and T2-weighted images (Fig. 3a–c). In turn, subaxial spinal cord compression due to OPLL was not evident (Fig. 3a–c). A change in the intensity of the spinal cord on T2-weighted images was also identified at the level of C1/2 (Fig. 3b).

Taking all of these findings into account, we attributed cervical myelopathy to the calcification of the posterior atlantoaxial membrane and posterior decompression surgery was performed. After bilateral exposure of C1/2, en-block extirpation of the posterior atlantoaxial membrane including the left calcified lesion was performed with partial laminectomy of C2, whereas we were able to preserve the posterior arch of C1. At the surgery, the lesion was carefully dissected from the dura matter. Chalky white deposits within the degenerated posterior atlantoaxial membrane were confirmed (Fig. 4a). Extensor muscles dissected from C2 were reconstructed after the decompression as much as possible. Histopathological examination revealed that calcified granules within degenerated fibrous tissue were surrounded by macrophages (Fig. 4b). The calcified granules were Alizarin red S positive (Fig. 4c). Furthermore, Raman

Published online: 08 September 2014

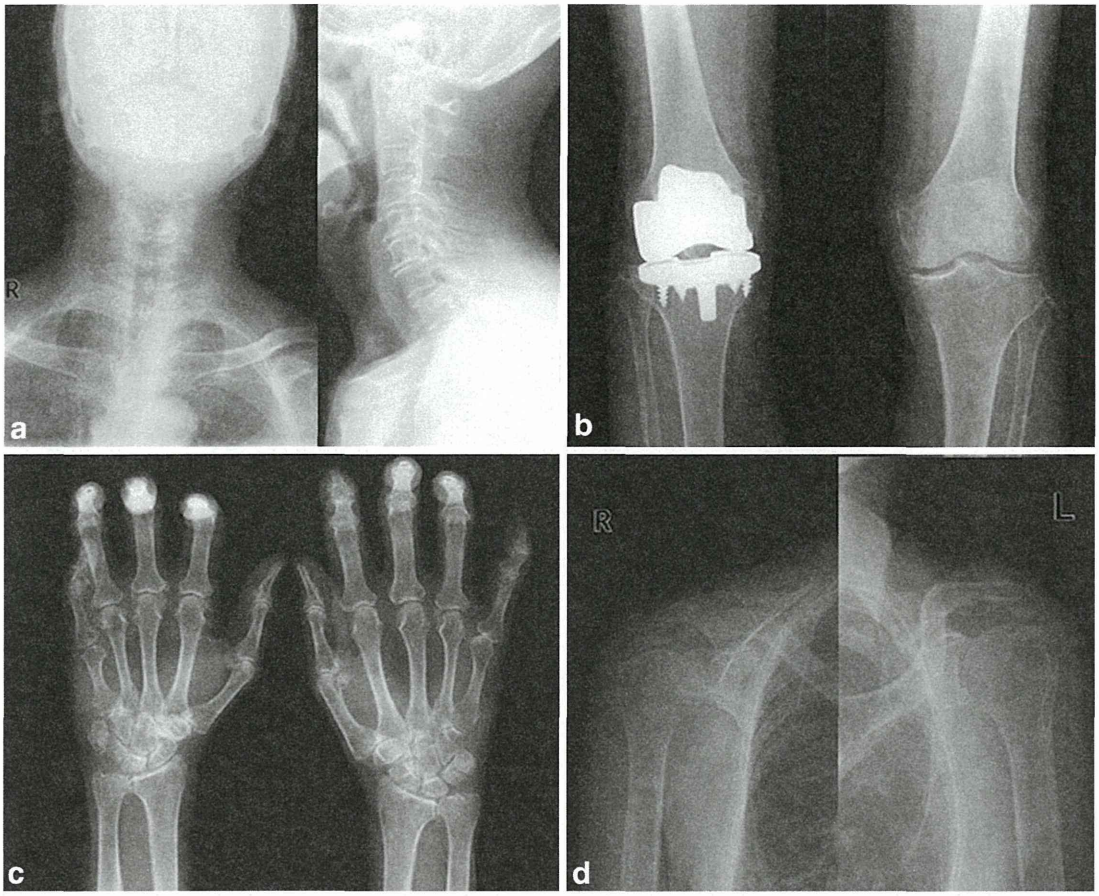

Fig. 1 Standard X-rays. **a** Ossification of the posterior longitudinal ligament of the cervical spine and an oval mass between the posterior arch of C1 and the lamina of C2 were confirmed. **b–d** Generalized articular calcifications were also seen

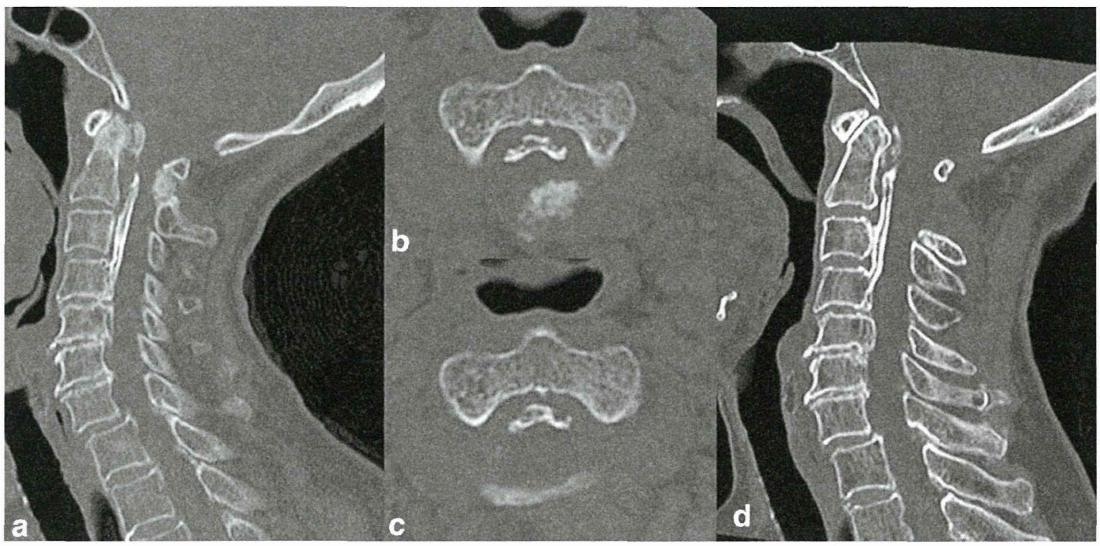

Fig. 2 **a, b** Pre-operative computed tomography (CT) revealed ossification of the longitudinal ligament of the spine extending from C2 to C5 and calcification at the posterior atlantoaxial membrane and retro-odontoid space. **c, d** Post-operative CT revealed extirpation of the calcification of the posterior atlantoaxial membrane

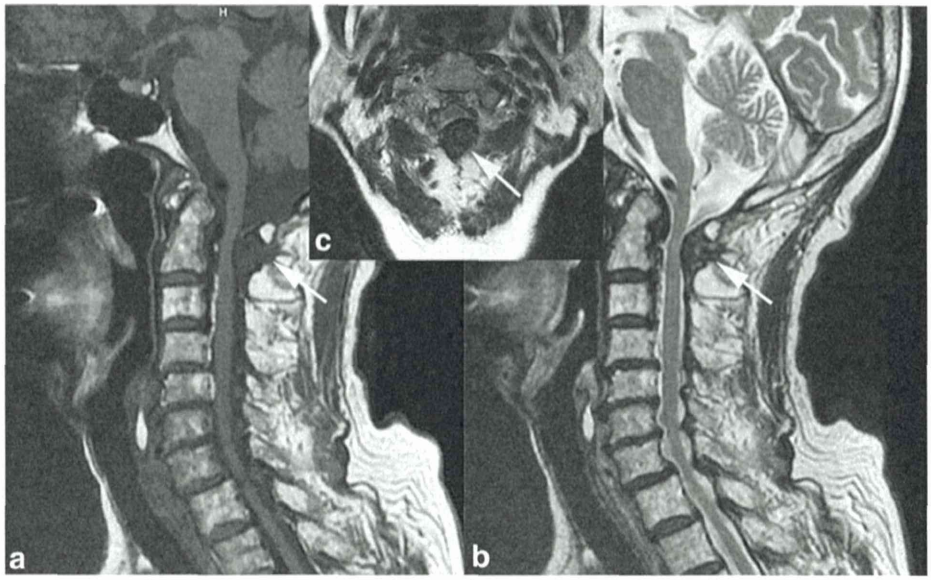

Fig. 3 Pre-operative magnetic resonance imaging demonstrated overt compression of the spinal cord due to calcification of the posterior atlantoaxial membrane (**c**), which was low intensity on both T1- (**a**) and T2-weighted (**b**) images (*arrows*), as well as a change in the intensity of the spinal cord on the T2-weighted image

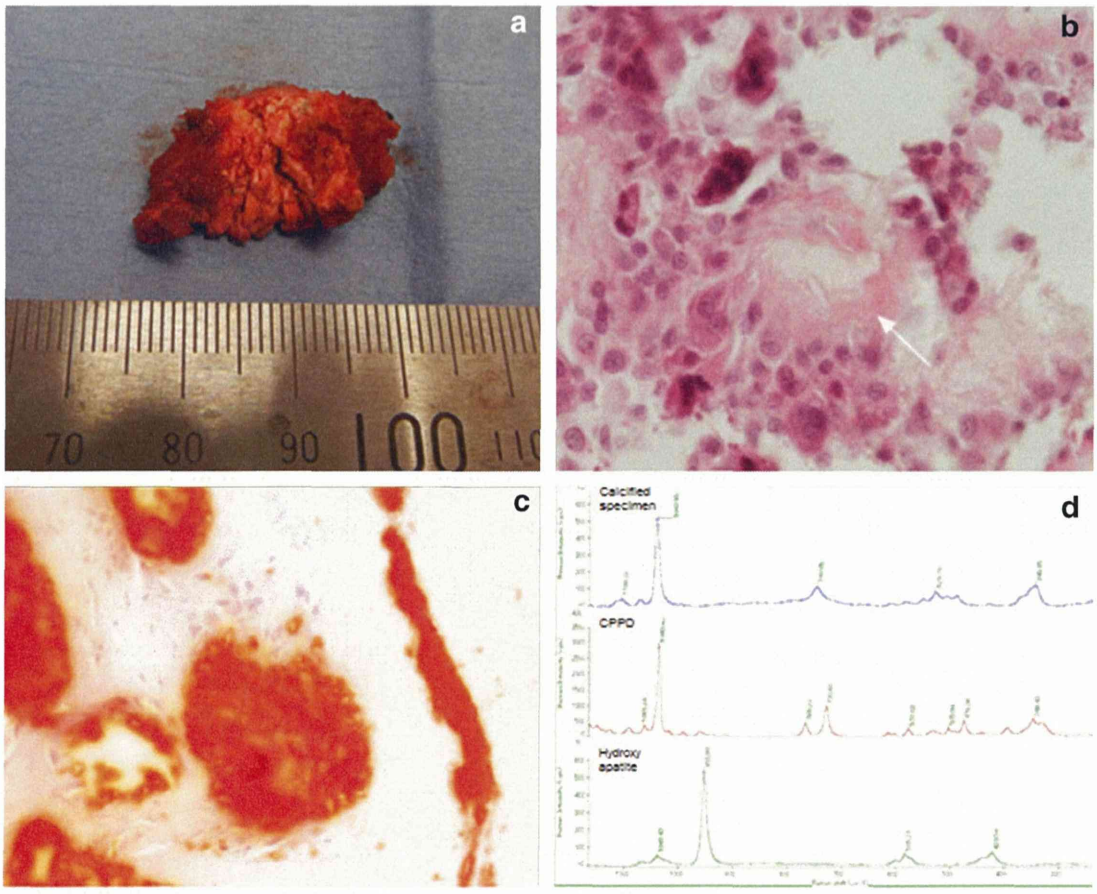

Fig. 4 **a** The presence of marked chalky white matter in the posterior atlantoaxial membrane was confirmed. **b** Histopathological examination revealed calcium pyrophosphate dihydrate (CPPD) crystals surrounded by macrophages (*arrow*, Original maginification ×400, H&E). **c** The calcified granules were positive for Alizarin red S staining (Original maginification×400). **d** Raman spectroscopy analysis revealed that the calcified lesion consisted only of CPPD, not hydroxy apatite